

1 **BioRT-Flux-PIHM v1.0: a watershed biogeochemical reactive transport**  
2 **model**

3 Wei Zhi<sup>1</sup>, Yuning Shi<sup>2</sup>, Hang Wen<sup>1</sup>, Leila Saberi<sup>3</sup>, Gene-Hua Crystal Ng<sup>3</sup>, Kayalvizhi  
4 Sadayappan<sup>1</sup>, Devon Kerins<sup>1</sup>, Bryn Stewart<sup>1</sup>, Li Li<sup>1,\*</sup>

5 <sup>1</sup> Department of Civil and Environmental Engineering, The Pennsylvania State University, State  
6 College, PA 16802, USA

7 <sup>2</sup> Department of Ecosystem Science and Management, The Pennsylvania State University, State  
8 College, PA 16802, USA

9 <sup>3</sup> Department of Earth and Environmental Sciences, University of Minnesota, Twin Cities, MN  
10 55455, USA

11 \* Correspondence to [lili@enr.psu.edu](mailto:lili@enr.psu.edu)

## Abstract

Watersheds are the fundamental Earth surface functioning ~~unit~~units that ~~connects~~connect the land to aquatic systems. Many watershed-scale models represent hydrological processes but ~~often~~ lack the representation of multi-component reactive transport processes ~~that are relevant to soil and aquatic biogeochemical reactions. The lack of mechanism-based representation of reaction thermodynamics and kinetics at the watershed scale.~~ This has limited our ~~ability~~capability to understand and predict solute export ~~and, water quality, particularly under~~chemistry, and earth system response to changing climate and anthropogenic conditions. Here we present a recently developed BioRT-Flux-PIHM (BioRT hereafter) v1.0, a watershed-scale biogeochemical reactive transport model. ~~Augmenting~~The model augments the previously developed RT-Flux-PIHM that integrates land-surface interactions, surface hydrology, and abiotic geochemical reactions ~~(Bao et al., 2017, WRR), the new development.~~ It enables the simulation of 1) shallow and deep water partitioning to represent surface water, shallow soil water, and deeper groundwater; 2) biotic processes including plant uptake, soil respiration, and microbially mediated reactions such as carbon decomposition and nutrient transformation; and 2) shallow and deep water partitioning to represent surface, shallow groundwater, and deep groundwater interactions.nutrient transformation. The reactive transport part of the code has been verified against the widely used reactive transport code CrunchTope. BioRT-Flux-PIHM v1.0 has recently been applied ~~to~~ ~~understand reactive transport processes~~ in multiple watersheds under diverse climate, vegetation, and geological conditions. This paper briefly introduces the governing equations and model structure with a focus on new model developments. It also showcases one hydrology example that simulates shallow and deep water interactions, and two biogeochemical examples relevant to nitrate and dissolved organic carbon (DOC). These examples are illustrated in two simulation modes of varying complexity. One is the spatially lumped mode (i.e., two land cells connected by one river segment) that focuses on processes and average behavior of a watershed. Another is the spatially distributed mode (i.e., hundreds of cells) that includes details of topography, land cover, and soil ~~property conditions.~~ The properties. Whereas the spatially lumped mode represents more of averaged properties and processes and temporal variations, the

- 43 spatially distributed mode can be used to understand the impacts of spatial structure and
- 44 identify hot spots of biogeochemical reactions.

## 45 1. Introduction

46 Watersheds are the fundamental Earth surface units that receive and process  
47 water, mass, and energy (Li, 2019; Li et al., 2020; ~~Ranalli and Macalady, 2010;~~ Hubbard et  
48 al., 2018; ~~Seyfried et al., 2018~~). Watershed processes include land surface interactions  
49 that regulate evapotranspiration and discharge, and water partitioning between shallow  
50 soil lateral flow going into streams versus downward flow and recharge into the deeper  
51 subsurface (~~Edwards et al., 2015~~) (~~Figure 1~~). ~~Complex biogeochemical interactions also~~  
52 ~~occur among soil, water, roots, and microbes, dictating gas effluxes (e.g., CO<sub>2</sub>) via soil~~  
53 ~~respiration, export of solute products derived from chemical weathering and~~  
54 ~~biogeochemical transformation~~ (~~Figure 1~~). Complex biogeochemical interactions occur  
55 among soil, water, roots, and microbes along water's flow paths, regulating gas effluxes  
56 (e.g., CO<sub>2</sub>) and solute export (Fatichi et al., 2019; van der Velde et al., 2010; Grathwohl et  
57 al., 2013).

58 These hydrological and biogeochemical processes determine how land Earth  
59 surface responds systems respond to ~~external forcings such as~~ hydroclimatic  
60 ~~drivers~~ forcing and human perturbations (van der Velde et al., 2014; Miller et al., 2020; Han  
61 et al., 2019; ~~Steimke et al., 2018~~). ~~Understanding these processes remains challenging~~  
62 ~~due to the complex coupling of land surface processes, hydrology, and biogeochemical~~  
63 ~~reactions~~ (~~Kirchner, 2003~~). Understanding these processes remains challenging due to  
64 the complex process interactions. An example is the concentration-discharge (C-Q)  
65 relationships of solutes at stream and river outlets. ~~These relationships encode the~~  
66 ~~integrated signature of land surface responses to changes in hydrological conditions~~  
67 (~~Brooks et al., 2015; Zhi et al., 2020; Zhi and Li, 2020~~). Similar C-Q relationships have  
68 been observed for some solutes across watersheds under diverse geological and climatic  
69 conditions (Godsey et al., 2009; Basu et al., 2010; Moatar et al., 2017; Zarnetske et al.,  
70 2018; Godsey et al., 2019), whereas different solutes have shown contrasting patterns in  
71 the same watershed (Miller et al., 2017; Herndon et al., 2015; ~~Zhi et al., 2019~~; Musolff et  
72 al., 2015). A general theory that can explain contrasting C-Q observations (e.g., flushing  
73 vs. dilution behaviors) under diverse watershed characteristics and forcing external  
74 conditions remains elusive. The lack of mechanistic understanding ~~of mechanisms~~

75 ~~governing hydrological and biogeochemical interactions~~ presents major roadblocks ~~for~~  
76 forecasting water quality, ~~including water issues such as eutrophication that persist~~  
77 ~~worldwide and earth system dynamics in the future.~~

78 One of the ~~outstanding~~ challenges ~~to answering questions relevant to water quality~~  
79 ~~and biogeochemical reactions~~ is the lack of modeling tools that mechanistically link  
80 hydrological and biogeochemical processes at the watershed scale. Model development  
81 has ~~been advancing separately~~ advanced mostly within the disciplinary boundaries of  
82 hydrology and biogeochemistry (Li, 2019). ~~Hydrologic~~ Watershed hydrologic models focus  
83 on solving for water storage and fluxes ~~at the watershed scale and beyond (Fatichi et al.,~~  
84 ~~2016).~~ (Fatichi et al., 2016). Reactive transport models (RTMs) have traditionally  
85 ~~centered~~ focused on transport and multi-component biogeochemical reactions  
86 ~~typically~~ mostly in groundwater systems, ~~which often have~~ with limited interactions with  
87 climate and other surficial ~~watershed processes~~ conditions (Steeffel et al., 2015; Li et al.,  
88 2017b; Mayer et al., 2002). ~~Biogeochemical reactions in shallow soils that are often driven~~  
89 ~~by environmental factors such as soil temperature and moisture cannot be well simulated~~  
90 ~~in these models.~~

91 ~~Previous modeling works has shown some.~~ Some integration ~~across these two~~  
92 ~~lines crossing disciplinary boundaries did occur in recent years.~~ For example, SWAT (Soil  
93 & Water Assessment Tool) ~~(Gassman et al., 2007; Lam et al., 2010; Moriasi et al.,~~  
94 ~~2013; Neitsch et al., 2011)~~ includes has a version that couples with the groundwater model  
95 MODFLOW and ~~simulate~~ the surface water and groundwater quality model in RT3D  
96 (Bailey et al., 2017; Ochoa et al., 2020). CATHY (Catchment Hydrology) includes  
97 processes of pesticide decay (Gatell et al., 2019; Scudeler et al., 2016). ~~Some other~~  
98 ~~hydrological models, including~~ Hydrologiska Byråns Vattenbalansavdelning (HBV) and  
99 the Hydrological Predictions for the Environment (HYPE), ~~also~~ ] have modules that  
100 simulate processes relevant to nutrients and contaminants (Lindström et al.,  
101 2005; Lindström et al., 2010). While ~~many of~~ these models can simulate ~~reaction~~  
102 processes such leaching of nutrients from agriculture lands (Lindström et al.,  
103 2005; Lindström et al., 2010; Bailey et al., 2017), ~~most of them~~ they do not explicitly solve  
104 the multi-component reactive transport equations. In other words, ~~they have relatively~~

105 ~~crude representations of solute leaching out of element bulk mass as part of the solute~~  
106 ~~export but do not represent~~ reactions are often represented rudimentarily without honoring  
107 kinetics and thermodynamics ~~of multi-component biogeochemical reactions typically~~  
108 ~~included theories~~ in ~~reactive transport models (RTMs)~~. They also do not simulate  
109 ~~processes such as chemical weathering. As an~~ soil biogeochemistry and geochemistry.  
110 For example, nutrient leaching is ~~often~~ calculated based on empirical equations without  
111 explicitly solving reactive transport equations. Reaction rates are ~~often~~ represented using  
112 first-order decay (Gatell et al., 2019), assuming constant reaction ~~rate constants~~ rates that  
113 do not change with ~~time~~ ~~and~~ environmental conditions. ~~However,~~  
114 ~~biogeochemical~~ Biogeochemical processes ~~including carbon decomposition and nutrient~~  
115 ~~cycling~~ however are highly variable ~~in space~~ with seasonal dynamics and ~~time,~~  
116 ~~depending~~ depend on local environments such as substrate availability, soil temperature,  
117 and soil moisture (Li et al., 2017a; ~~Suseela et al., 2012;~~ HARTLEY et al., 2007). ~~In filling in~~  
118 ~~this model need, recently we augmented our watershed model RT-Flux-PIHM (Bao et al.,~~  
119 ~~2017) with new developments of microbially mediated reactions, which allows us to model~~  
120 ~~the interactions between biogeochemical reactions and environmental factors that are~~  
121 ~~driven by land surface and hydrological processes.~~ These models therefore cannot  
122 capture the temporal variations in environmental factors that regulate soil biogeochemical  
123 reactions and stream and water chemistry.

124 ~~————~~ To fill this model capability need, we augmented  
125 the watershed model RT-Flux-PIHM (Bao et al., 2017) into BioRT-Flux-PIHM (BioRT  
126 hereafter) ~~v1.0, augmented based on~~. Compared to RT-Flux-PIHM ~~with,~~ BioRT has two  
127 ~~new~~ additions. One is the capability of simulating biotic processes including plant uptake  
128 of nutrients, soil respiration, and ~~microbially~~ other microbe-mediated redox reactions ~~in~~  
129 ~~the soil~~. Examples include ~~the~~ soil respiration that produces CO<sub>2</sub> and ~~carbon~~  
130 ~~decomposition that generates~~ dissolved organic carbon (DOC), and ~~other~~ nutrient  
131 transformation ~~processes~~ reactions such as nitrification and denitrification. The other is  
132 the ~~introduction~~ addition of an optional deeper layer below ~~the~~ shallow soil ~~that enablesto~~  
133 enable the simulation of ~~interactions of~~ interacting deep water and shallow soil water flow  
134 (Figure 1). Here the deep water is loosely defined as the water ~~beyond~~ below the soil  
135 zone, typically in less weathered, fractured subsurface that harbors relatively old and

136 slow-moving groundwater contributing to streams. ~~This contrasts with shallow water in~~  
137 ~~highly permeable soils. Mounting evidence~~ It is a fundamental component of the  
138 hydrologic cycle and water budget. The groundwater-surface water interactions also  
139 modulate land-atmospheric energy exchanges and soil moisture dynamics (Keune et al.,  
140 2016). Evidence has been mounting in recent years ~~has shown~~ that deeper water  
141 ~~beyond~~ below the shallow soil interacts with streams, introduces water with distinct  
142 chemistry, sustains base flow in dry times, and buffers climate variability (Gurdak,  
143 2017;Green, 2016;Taylor et al., 2013;~~Gendon et al., 2013;Anyah et al., 2008;Maxwell et~~  
144 ~~al., 2011;Gleeson et al., 2015~~). Stream chemistry often reflects ~~the~~ distinct chemistry from  
145 ~~the~~ shallow soil water and deeper groundwater ~~zones~~ at different time, i.e., the so called  
146 Shallow and Deep Hypothesis (Zhi et al., 2019;Zhi and Li, 2020;~~Botter et al., 2020~~).  
147 ~~Deeper groundwater is thus a fundamental component of the hydrologic cycle and water~~  
148 ~~budget. The groundwater-surface water interactions can also modulate land-atmospheric~~  
149 ~~energy exchanges and soil moisture dynamics (Keune et al., 2016;Martínez-de la Torre~~  
150 ~~and Miguez-Macho, 2019).~~ Including the deep water component thus ~~enables the~~  
151 ~~simulation of such interactions and the~~ is essential for understanding mechanisms and  
152 predicting dynamics of water quality ~~under changing climate and human conditions.~~

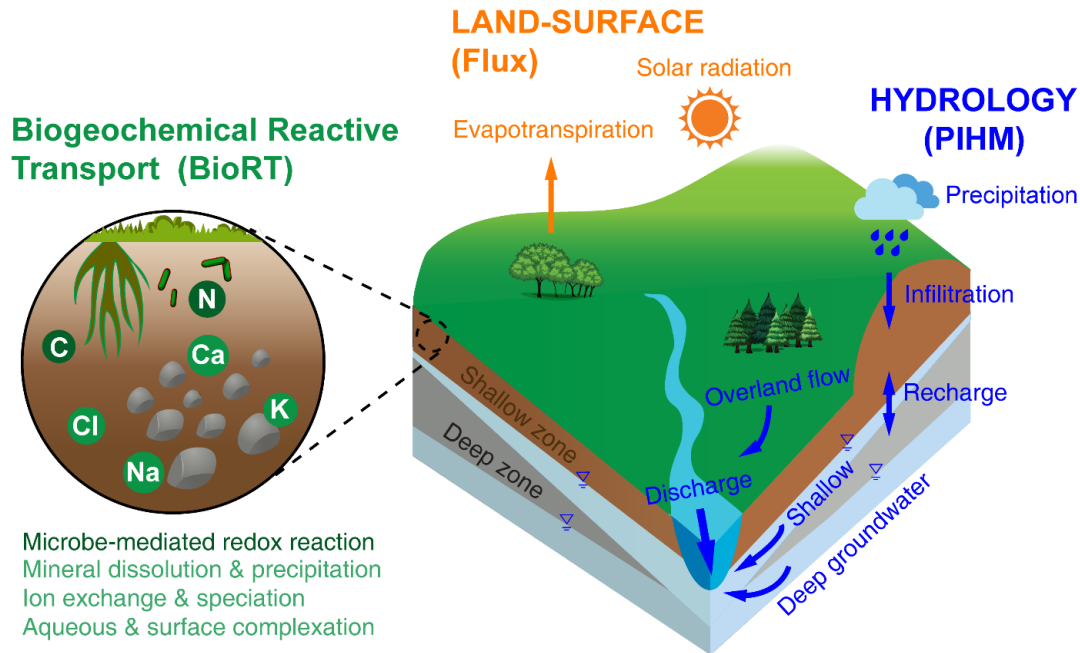
153 This paper introduces the new developments in ~~the~~ BioRT ~~model~~. The ~~code~~ ~~has~~  
154 ~~been verified against the widely used reactive transport code CrunchTope (Supporting~~  
155 ~~Information, SI). This paper briefly overviews~~ starts with a brief overview of water and  
156 energy related processes ~~incorporated in the model. Readers are referred to previous~~  
157 ~~publications for more details of processes such as evapotranspiration (ET), hydrological~~  
158 ~~flow, and abiotic reactions (Shi et al., 2013;Bao et al., 2017;Li et al., 2017a;Qu and Duffy,~~  
159 ~~2007). We showcase.~~ It then introduces governing equations and reaction kinetics used  
160 in BioRT, followed by three examples that illustrate the new ~~model~~ capabilities ~~and the~~  
161 ~~simulation of biogeochemical reactions.~~ The first hydrological example ~~show~~ examples  
162 include the surface water and groundwater interactions. ~~This second example focuses~~  
163 ~~on,~~ nitrate transformation and transport ~~in a spatially lumped mode. The third example~~  
164 ~~examines the,~~ and the production and export of DOC ~~with the representation of spatial~~  
165 ~~details.~~ The model can be set up in both spatially lumped or spatially explicit modes. The

166 source code and the examples shown here are hosted on the GitHub website  
167 (<https://github.com/PSUmodelingLi-Reactive-Water-Group/BioRT-Flux-PIHM>).  
168

## 169 **2. Model overview**

170 BioRT-Flux-PIHM integrates three modules (Figure 1). The Flux module is for land-  
171 surface processes including surface energy balance, solar radiation, and ET (Shi et al.,  
172 2013). The hydrology module PIHM simulates water processes including precipitation,  
173 interception, infiltration, recharge, surface runoff, subsurface lateral flow, and deep water  
174 flow (Qu and Duffy, 2007). The BioRT module simulates solute transport, ~~bio-relevant  
175 processes such as plant uptake of nutrients from water, and multi-component~~ reactions.  
176 The ~~reaction processes can include soil respiration, microbially mediated redox abiotic  
177 reactions (e.g., soil respiration, carbon decomposition and nutrient transformation), ion  
178 exchange, aqueous and surface complexation, and mineral dissolution and precipitation.~~  
179 ~~Note that geochemical reactions included in our previous RT-Flux-PIHM are abiotic~~ (Bao  
180 et al., 2017), ~~including are~~ mineral dissolution and precipitation, aqueous and surface  
181 complexation, and ion exchange reactions. The newly added reactions include plant  
182 uptake of nutrients, soil respiration, microbe-mediated redox reactions (e.g., carbon  
183 decomposition and nutrient transformation).





184

185 **Figure 1.** A conceptual diagram for processes at the watershed scale. ~~This includes land~~  
 186 ~~surface interactions~~ include processes such as energy balance, solar radiation, and  
 187 ~~evapotranspiration~~ ~~(e.g., evaporation, transpiration, and snow sublimation)~~; hydrological  
 188 processes partitioning/partition water between surface runoff, shallow soil water, and deeper water  
 189 entering the stream. Soil biogeochemical reactions include abiotic reactions such as weathering  
 190 ~~(e.g., mineral dissolution and precipitation)~~, ion exchange, surface complexations), and biotic  
 191 processes such as ~~soil respiration~~, plant uptake of nutrients, soil respiration, and other microbe-  
 192 mediated reactions ~~such as transformation of carbon and nitrogen~~. These processes are  
 193 represented in three modules: The Flux module for land-surface interactions, the PIHM module  
 194 for catchment hydrology, and the ~~recently augmented~~ BioRT module for biogeochemical  
 195 reactions. Conceptually the shallow zone is the shallow soil and weathered zone that are more  
 196 conductive to water flow (e.g., soil lateral flow or interflow). The deep zone refers to the less  
 197 weathered zone that often harbors the ~~relatively~~ old and slow flowing groundwater. Reactions can  
 198 occur in both shallow and deep zones. ~~For the BioRT, the light and dark greens refer to abiotic~~  
 199 ~~and biological reactions, respectively.~~

200

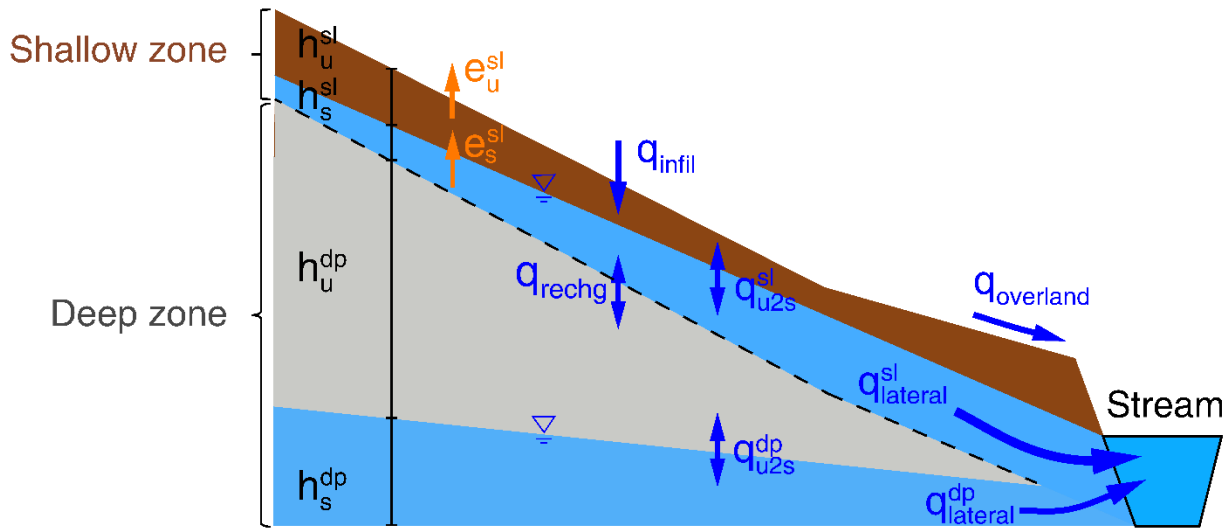
201 The land surface and hydrology modules solve for soil temperature and water  
 202 storage, from which water fluxes ~~can be quantified~~ are calculated for surface runoff,  
 203 shallow and deep water fluxes. The BioRT module uses the calculated soil temperature,  
 204 water storage, and water fluxes to simulate ~~advection, diffusion/dispersion, solute~~  
 205 transport (advective and diffusive/dispersive) and biogeochemical reactions in both  
 206 shallow and deep zones (see governing equations in later sections). The reactions ~~can~~

207 ~~be~~include kinetically controlled (e.g., ~~microbial~~microbe-mediated redox reaction, mineral  
208 dissolution and precipitation) or equilibrium-controlled (e.g., ion exchange, surface  
209 complexation (sorption), and aqueous complexation). Users can define the types of  
210 reactions to be included and the form of reaction kinetics in input files. The output of  
211 BioRT includes the spatial distribution and time series of aqueous and solid  
212 concentrations, from which we can ~~also~~ infer reaction rates.

213 ~~The simulation domain is~~The model can be set up running in either spatially  
214 lumped or spatially explicit modes. When running in spatially explicit mode, the simulation  
215 domain can be structured as prismatic grids based on topography. Each grid is partitioned  
216 into surface and shallow and deep subsurface layers. The surface layer calculates water  
217 flow above ground (surface runoff). The shallow zone is loosely defined as the highly  
218 permeable subsurface that ~~is contrasting to~~contrasts the deep zone that is broadly  
219 defined as the lower permeability zone beyond the shallow zone. In many places, ~~this~~the  
220 shallow zone is the soil zone that is most conducive to water flow (e.g., ~~soil~~-lateral flow)  
221 and is responsive to hydroclimatic ~~forcings~~forcing. The deep subsurface zone is the less  
222 weathered layer that harbors the ~~relatively older and slower flowing~~old ground water that  
223 contributes to stream flow. Note that these definitions differ from those in the hydrology  
224 community, which often refers to the shallow soil ~~water~~lateral flow ~~or lumped shallow soil~~  
225 as groundwater, in a way that distinguishes it from the surface runoff (~~Winter et al.,~~  
226 ~~1998; Dingman, 2015; Todd and Mays, 2005~~); (Dingman, 2015). These ~~shallow and~~  
227 ~~deep~~source waters from different depths of the subsurface often have distinct solid and  
228 water chemistry, and are dominant at different hydrological conditions in different time of  
229 the year, as have been observed ~~and inferred~~ in many catchments and watersheds  
230 (~~Brantley et al., 2018; Zhi et al., 2019; Zhi and Li, 2020; Li et al., 2020; Sullivan et al., 2016~~);  
231 ~~Despite the model complexity, the~~ The model is flexible for taking inputs from online data  
232 portals or local measurements and it can accommodate low data availability (see the  
233 following section of 5 for data need and domain setup). ~~The model is developed as a~~  
234 ~~research tool to understand coupled watershed processes rather than as a policy model~~  
235 ~~to guide management.~~

236

237 **3. Governing equations and processes**



238  
 239 **Figure 2.** Hillslope view of the shallow and deep zones and relevant water flows. Streams  
 240 received water primarily from three water flows: the surface runoff ( $q_{overland}$ ), and lateral flow from  
 241 shallow zone ( $q_{lateral}^{sl}$ ), and the lateral flow that has been recharged and eventually come out from  
 242 deeper zone ( $q_{lateral}^{dp}$ ). The symbol of “h”, “e”, and “q” denotes water storage—[m],  
 243 evapotranspiration—[m/s], and water flow—[m/s], respectively. The superscript letter “sl” and “dp”  
 244 refer to shallow and deep zone, respectively. The subscript letters “u” and “s” refer to unsaturated  
 245 and saturated layerlayers, respectively. Detailed equations are listed—in the following  
 246 sectionssection 3.1 – 3.2. The terms “infil”, “u2s”, and “recharge” refer to infiltration, unsaturated  
 247 to saturated zones, and recharge.

248  
 249 **3.1 Water equations**

250 The original Flux-PIHM simulates surface runoff and a lumped subsurface flux into  
 251 streams without distinguishing shallow soil water flow and deeper groundwater flow. In  
 252 working with stream water chemistry data, we realized paths. Mounting evidence has  
 253 shown that a lumped subsurface flow cannot describe the dynamics of stream chemistry,  
 254 as the shallow soil water and deeper groundwater have distinct chemistry and are  
 255 dominant at different times of the year (Zhi et al., 2019; Zhi and Li, 2020). (Xiao et al.,  
 256 2021; Zhi and Li, 2020; Zhi et al., 2019). This means that a lumped subsurface flow cannot  
 257 describe the dynamics of stream chemistry. We therefore added an optional deeper  
 258 groundwater zone in the code to simulate the deeper water flows that interactsinteract

259 with streams. Each prismatic element now has three zones in the vertical direction:  
 260 surface (or above ground), shallow and deep zones in the subsurface.

261 In each prismatic element  $i$ , the shallow zone includes unsaturated and saturated  
 262 water storages. The unsaturated zone receives water from the surface via infiltration and  
 263 ~~only~~ flows vertically to the saturated zone. The saturated zone flows both vertically to the  
 264 deep zone (recharge) and laterally to neighboring grids  $j$  or the stream (lateral). The code  
 265 solves the following equations ~~for~~in the shallow zone:

$$266 \quad \theta_i^{sl} \frac{dh_{i,u}^{sl}}{dt} = q_{i,inf} - q_{i,u2s}^{sl} - e_{i,u}^{sl} \quad (1)$$

$$267 \quad \theta_i^{sl} \frac{dh_{i,s}^{sl}}{dt} = q_{i,u2s}^{sl} - q_{i,rechg} - e_{i,s}^{sl} + \sum_1^{N_{ij}} q_{ij}^{sl} \quad (2)$$

268 Where  $\theta_i^{sl}$  [m<sup>3</sup> pore space/m<sup>3</sup> total volume] is the shallow zone porosity in ~~the~~ element  $i$ ;  
 269  $h_{i,u}^{sl}$  and  $h_{i,s}^{sl}$  [m] are the unsaturated and saturated water storage in the shallow zone,  
 270 respectively. ~~Note that the~~The storages  $h$  here are ~~essentially~~ the height of soil column  
 271 with equivalent saturated water, not the height of the pure water (100% volume) column.  
 272 That is why porosity is in the equation. For saturation zones, this height is needed to  
 273 quantify the depths of water tables and determines the direction of water flow between  
 274 neighboring grids. The  $q_{i,inf}$  [m/s] is the infiltration rate from the surface to the shallow  
 275 zone;  $q_{i,u2s}^{sl}$  [m/s] is the vertical flow from the unsaturated layer to the saturated layer in  
 276 the shallow zone;  $q_{i,rechg}$  [m/s] is the recharge rate from the shallow zone to the deep  
 277 zone;  $e_{i,u}^{sl}$  and  $e_{i,s}^{sl}$  [m/s] are evapotranspiration (ET) from the unsaturated and saturated  
 278 layer in the shallow zone, respectively;  $q_{ij}^{sl}$  [m/s] are the lateral flows in the shallow  
 279 saturated layer between the element  $i$  and its neighbor element  $j$ ;  $N_{ij}$  ( $\leq 3$ ) is the number  
 280 of neighbor elements  $j$ . For a prismatic element  $i$ , a boundary cell ~~could have~~has one or  
 281 two neighbors; a non-boundary cell has three neighbors. ~~The~~ ET is calculated by the  
 282 Penman potential evaporation scheme ~~and~~ ~~(detailed equations can be found in Shi~~  
 283 ~~(2012); Shi (2012))~~. A similar set of water equations for the deep zone are in the SI (Eqn.  
 284 S1 and S2).

Infiltration and vertical fluxes from the unsaturated to ~~the~~ saturated layer in the shallow zone are based on the Richards equation, in which hydraulic water head  $H$  (i.e., the summation of water storage  $h$  and elevation head  $z$ ) and hydraulic conductivity  $K$  ~~are used to~~ determine the fluxes ~~in each element  $i$ :~~

$$q_{i,inf} = K_{i,inf} \frac{H_{i,sur} - H_{i,u}^{sl}}{d_{i,inf}} \quad (3)$$

$$q_{i,u2s}^{sl} = K_{i,v}^{sl} \frac{H_{i,u}^{sl} - H_{i,s}^{sl}}{0.5d_i^{sl}} \quad (4)$$

Where  $d_{i,inf}$  and  $d_i^{sl}$  [m] are the thickness of infiltration layer and shallow zone depth ~~for the elements  $i$ ,~~ respectively;  $K_{i,inf}$  [m/s] is the hydraulic conductivity of the infiltration layer, the top 0.1 m of the subsurface ~~and is considered to have that has~~ different conductivity from the rest of subsurface;  $K_{i,v}^{sl}$  [m/s] is the hydraulic conductivity in the vertical direction (i.e., weighted average of macropore  $K_{i,macv}$  and soil matrix  $K_{i,satv}$ , Eqn. S7);  $H_{i,sur}$  [m] is the surface hydraulic water head ( $= h_{i,sur} + z_{i,sur}$ );  $H_{i,u}^{sl}$  and  $H_{i,s}^{sl}$  [m] are the shallow hydraulic water heads in the unsaturated and saturated layer, respectively. The lateral flow in the shallow saturated layer is calculated using Darcy's law:

$$q_{ij}^{sl} = K_{ij}^{sl} \frac{H_{i,s}^{sl} - H_{j,s}^{sl}}{d_{ij}} \quad (5)$$

Where  $d_{ij}$  [m] is the distance between the centers of elements  $i$  and  $j$ ;  $K_{ij}^{sl}$  [m/s] is the harmonic mean of shallow hydraulic conductivity in the horizontal direction between elements  $i$  ( $K_{i,H}^{sl}$ ) and  $j$  ( $K_{j,H}^{sl}$ ). The interaction between the shallow saturated zone and stream channel also follows Eqn. 5, except that the adjacent head is replaced by the level of ~~the channel stream~~ water. Similar to the shallow zone, hydrological equations in the deep zone are detailed in the SI (Eqn. S1 – S8).

### 3.2 Reactive transport equations

The governing advection dispersion reaction (ADR) equation for an arbitrary solute  $m$  in ~~grid  $i$  is as follows (Bao et al., 2017), i.e., the change of solute mass (i.e., the left~~

310 ~~term in Eqn. 6) is driven by dispersive transport, advective transport, and reactions (i.e.,~~  
 311 ~~the 1<sup>st</sup>, 2<sup>nd</sup>, and 3<sup>rd</sup> right-hand side terms, respectively)~~ an element  $i$  is as follows (Bao et  
 312 al., 2017):

$$313 \quad V_i \frac{d(S_{w,i} \theta_i C_{m,i})}{dt} = \sum_1^{N_{ij}} \left( A_{ij} D_{ij} \frac{C_{m,j} - C_{m,i}}{d_{ij}} - q_{ij} A_{ij} C_{m,j} \right) + R_{m,i}, \quad m = 1, \dots, nm \quad (6)$$

314 Where  $V_i$  [m<sup>3</sup> total volume] is the total volume of element  $i$ ;  $S_{w,i}$  [m<sup>3</sup> water/m<sup>3</sup> pore space]  
 315 is soil water saturation;  $\theta_i$  [m<sup>3</sup> pore space/m<sup>3</sup> total volume] is the porosity;  $C_{m,i}$  [mol/m<sup>3</sup>  
 316 water] is the aqueous concentration of species  $m$ ;  $N_{ij}$  is the number of fluxes from  
 317 neighbor element  $j$  for element  $i$ ,  $N_{ij}$  is 2 for the unsaturated zone (infiltration, recharge)  
 318 with only vertical flows and 5 for saturated zone with flux from (or to) the unsaturated  
 319 zone, from (or to) the deeper zone, and fluxes between  $i$  and three neighbor elements  $j$   
 320 in lateral flow directions for non-boundary grids;  $A_{ij}$  [m<sup>2</sup>] is the grid area shared by  $i$  and  
 321 its neighbor grid  $j$ ;  $D_{ij}$  [m<sup>2</sup>/s] is the hydrodynamic dispersion coefficient (i.e., sum of  
 322 mechanical dispersion and effective diffusion coefficient) normal to the shared surface  
 323  $A_{ij}$ ;  $d_{ij}$  [m] is the distance between the center of  $i$  and its neighbor elements  $j$ ;  $q_{ij}$  [m/s]  
 324 is the flow rate across  $A_{ij}$ ;  $R_{m,i}$  [mol/s] is the total rate of kinetically controlled reactions in  
 325 element  $i$  that involve species  $m$ ;  $nm$  is the total number of independent primary species  
 326 to be solved for reactive transport equations. Equation (6) states that the change of solute  
 327 mass (the left term) is driven by dispersive transport, advective transport, and reactions  
 328 (i.e., the 1<sup>st</sup>, 2<sup>nd</sup>, and 3<sup>rd</sup> right-hand side terms, respectively).

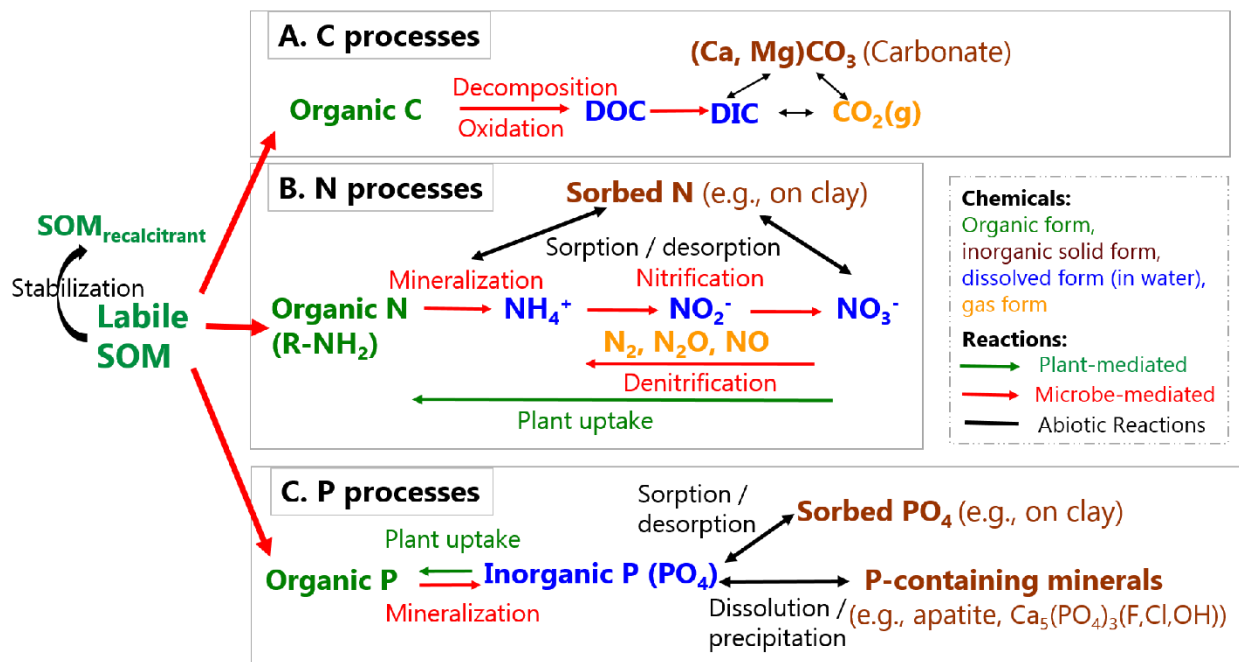
329

### 330 **3.3 Biogeochemical processes and reaction kinetics**

#### 331 **3.3.1 Biogeochemical processes**

332 Here we discuss ~~some~~ representative biogeochemical processes that involve  
 333 plants and microbes that can be included in BioRT. BioRT differs from general water  
 334 quality models that ~~often~~ primarily target a few contaminants (e.g., N, P, metals). The  
 335 framework of ~~the code~~ BioRT is flexible and the users can define ~~their~~ reactions and  
 336 solutes of interests in the input files. For abiotic reactions such as mineral dissolution and  
 337 surface complexation or ion exchange, readers are referred to ~~an earlier paper~~ (Bao et

338 al. (2017). Generally speaking, shallow soils ~~compared to deep soils~~ contain more  
 339 weathered materials and soil organic matters (SOM) including roots, leaves, and  
 340 microbes. SOM can be decomposed partially into organic molecules that dissolve in water  
 341 (~~Wieder et al., 2015~~), i.e., DOC, or it can be ~~oxidized completely into CO<sub>2</sub> that is released~~  
 342 ~~back to the atmosphere as a gas, i.e., Dissolved Organic Carbon (DOC). It can also~~  
 343 ~~become oxidized completely into CO<sub>2</sub>, which can emit back to the atmosphere in gas~~  
 344 ~~form~~ (Davidson, 2006) or ~~surface water transport and enter streams~~ in the form of  
 345 dissolved inorganic carbon (DIC). With coexisting cations (e.g., Ca, Mg), DIC can ~~often~~  
 346 precipitate out and become carbonate minerals (e.g., CaCO<sub>3</sub>).



347  
 348 **Figure 3.** Biotic and abiotic reactions relevant to the transformation of soil organic matter (SOM).  
 349 ~~#SOM~~ can become stabilized (recalcitrant) through sorption on clay and separation from  
 350 reactants. Labile OM can decompose into inorganic forms, releasing C, N, and P that further  
 351 transform ~~between different into various~~ forms (adopted from Li (2019), permission with  
 352 Mineralogical Society of America).

353  
 354 OM decomposition releases organic nitrogen (R-NH<sub>2</sub>), which can further react to  
 355 become NH<sub>4</sub><sup>+</sup> and other nitrogen forms (N<sub>2</sub>, N<sub>2</sub>O, NO, NO<sub>2</sub><sup>-</sup>, NO<sub>2</sub>) (Figure 3). The gases  
 356 can ~~be emitted~~ emit back to the atmosphere (~~Saha et al., 2017; Maavara et al., 2018~~).  
 357 Denitrification requires anoxic conditions and occurs less commonly in shallow soils  
 358 owing to the pervasive presence of O<sub>2</sub> (Sebestyen et al., 2019); ~~#denitrification~~ can

359 become important under wet conditions and in O<sub>2</sub>-depleted groundwater  
360 ~~systems~~aquifers. Phosphorous (P) can be in ~~an~~organic ~~form (e.g., leaves);~~forms in  
361 organic matter, sorbed on fine soil particles, dissolved in water, or in solid forms as P-  
362 containing minerals. Transformation of nutrients occurs through various bio-mediated or  
363 abiotic reactions. A representative P-containing mineral in the Earth's crust is apatite  
364 Ca<sub>5</sub>(PO<sub>4</sub>)<sub>3</sub>(F, Cl, OH). Once liberated via rock dissolution, P is ~~mostly~~biologically  
365 assimilated and locked in organic forms. These organic forms have very low solubility,  
366 allowing them to bind on and be transported together with soil particles in the form of  
367 orthophosphate or pyro-diphosphate. ~~Overall, these reactions are a combination of biotic~~  
368 ~~and abiotic reactions.~~

369

### 370 3.3.2 Reaction kinetics in natural soils

371 **Rate dependence on temperature and soil moisture.** Reactions such as soil  
372 respiration and plant uptake typically depend on environmental conditions (temperature  
373 or soil moisture). For example, in shallow oxic soils where organic carbon and O<sub>2</sub> are  
374 often abundant, the rate law for carbon decomposition can be simplified to the following  
375 form assuming microorganism concentrations are relatively constant.

376

$$r = kAf(T)f(S_w)f(Z_w) \quad (7)$$

377 Where the reaction rate  $r$  [mol/s] depends on rate constant  $k$  [mol/m<sup>2</sup>/s], the surface area  
378  $A$  [m<sup>2</sup>] is a lumped parameter that quantitatively represents SOM content and biomass  
379 abundance,  $f(T)$  and  $f(S_w)$  describe the temperature and soil moisture dependence,  
380 respectively,  $f(Z_w)$  can be included to account for the depth distribution of SOM (Seibert  
381 et al., 2009), and  $Z_w$  [m] is the water table depth. An example for the depth distribution is  
382  $f(Z_w) = \exp\left(-\frac{Z_w}{b_m}\right)$  (Weiler and McDonnell, 2006; ~~Ottey et al., 2016;~~Bai et al., 2016), with  
383  $b_m$  as the depth coefficient describing the gradient of SOM content over depth. Users can  
384 choose to include either one or all of these ~~dependences~~dependencies in input or  
385 database files.

386 The temperature dependence follows a Q<sub>10</sub>-based form (Lloyd and Taylor,  
387 1994;Friedlingstein et al., 2006;Hararuk et al., 2015) as follows:



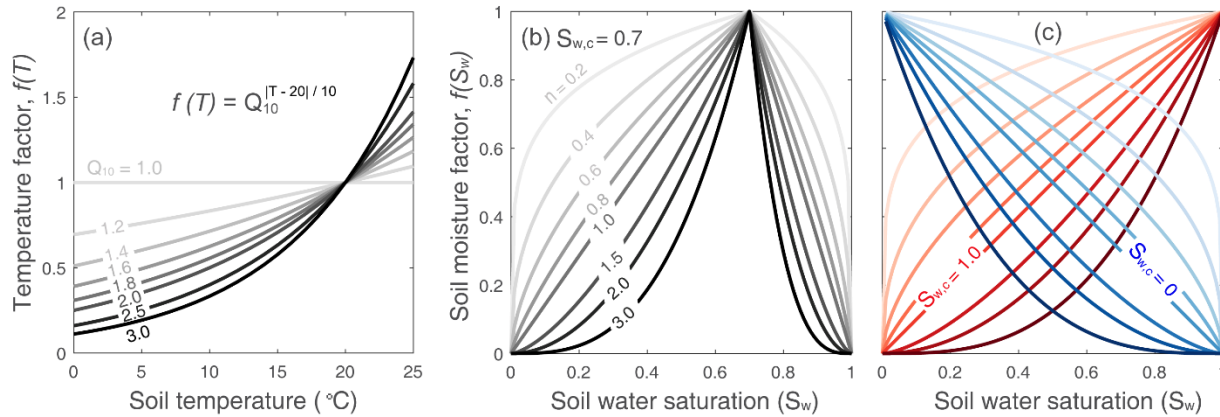
388 
$$f(T) = Q_{10}^{\frac{T-20}{10}} Q_{10}^{(T-20)/10} \quad (8),$$

389 where  $Q_{10}$  is the relative increase in reaction rates when temperature increases by 10 °C  
 390 (Davidson and Janssens, 2006). Values of  $Q_{10}$  (Figure 4a) can vary from 1.0 to 3.0,  
 391 depending on climatic conditions, substrate availability, and ecosystem type (e.g.,  
 392 grassland, forest) (Davidson et al., 2006; Liu et al., 2017) (Davidson et al., 2006; Liu et al.,  
 393 2017). The mean values are in the range of 1.4 to 2.5 (Zhou et al., 2009; Bracho et al.,  
 394 2016). The  $Q_{10}$  value can be specified in the input file. ~~The soil moisture dependence~~  
 395 ~~function  $f(S_w)$  is coded based on the following form:~~

396 The soil moisture dependence function  $f(S_w)$  is coded in the following form:

397 
$$\begin{cases} \left(\frac{S_w}{S_{w,c}}\right)^n, S_w \leq S_{w,c} \\ \left(\frac{1-S_w}{1-S_{w,c}}\right)^n, S_w > S_{w,c} \end{cases} \quad (9)$$

398 Here  $S_{w,c}$  [0 to 1] is the critical soil moisture at which rates are highest, and  $n$  is the  
 399 exponent reflecting the dependence of rates on soil moisture. A typical  $n$  value is 2 (Yan  
 400 et al., 2018) with a range between 1.2 and 3.0 (Hamamoto et al., 2010), depending on  
 401 soil structure and texture. As shown in Figure 4b, the form indicates an intermediate  
 402 critical soil moisture  $S_{w,c}$  at which  $f(S_w)$  reaches its maximum. When  $S_w$  ~~is below this~~  
 403 ~~value,  $\leq S_{w,c}$ ,  $f(S_w)$  increases with  $S_w$ ; when  $S_w$  is above this value,  $> S_{w,c}$ ,  $f(S_w)$~~   
 404 ~~decreases with  $S_w$ -behavior~~ (Figure 4b) (Yan et al., 2018). Under the extreme conditions  
 405 of  $S_{w,c}$  equals to 0 or 1,  $f(S_w)$  monotonically increase or decrease (Figure 4c). The two  
 406 parameters,  $S_{w,c}$  and  $n$ , determines the shape of the curve. They can be specified in input  
 407 or database files. One can also choose not to have temperature or soil moisture  
 408 dependence by choosing parameters that would lead to the value of exponent being zero.



409  
 410 **Figure 4. Reaction rate dependence.** (a) Function form of soil temperature dependence and (b,  
 411 c) soil moisture dependence for reaction rates. The ~~temperature factor  $f(T)$  is a function of~~  
 412 ~~the takes  $Q_{10}$  (defined by users) and soil temperature form (Equation 8).~~ The soil moisture factor  
 413  ~~$f(S_w)$  is a function of two user-defined parameters depends on  $S_{w,c}$  and  $n$  and soil water~~  
 414 ~~saturation  $S_w$  (Equation 9).~~ The soil moisture function can represent three types of behaviors: the  
 415 threshold behavior (b,  $0 < S_{w,c} < 1$ ), increase behavior (red in (c),  $S_{w,c} = 1$ ), and decrease  
 416 behavior (blue in (c),  $S_{w,c} = 0$ ). Values of  $n = 1$  leads to a linear threshold dependence of  $S_w$  while  
 417  $n < 1$  and  $n > 1$  lead to concave and convex dependences, respectively.

418  
 419 **Rate dependence on substrates: Monod kinetics and biogeochemical redox**  
 420 **ladder.** Deeper groundwater aquifers often experience anoxic conditions that lead to  
 421 processes such as denitrification or methanogenesis. This can also happen in wetlands  
 422 or wet soils. ~~The~~ Under such conditions, the rates of microbe-mediated redox reactions  
 423 depend not only on temperature and soil moisture as discussed above, they also depend  
 424 on concentrations of electron donors and non-oxygen electron acceptors (e.g., nitrate,  
 425 iron oxides, sulfate) that are often limited under anoxic conditions (Bao et al., 2014; Li,  
 426 2019; Benettin et al., 2020). The order of ~~the~~ redox reactions ~~often~~ typically follows the  
 427 biogeochemical redox ladder, which is based on how much microbe can harvest energy  
 428 by reducing different types of electron acceptors. Monod reaction rate laws are often used  
 429 for quantifying rates of these redox conditions. These rate laws are detailed in the section  
 430 S2 of Supporting Information ~~and also in Li (2019).~~ Users can combine these Monod rate  
 431 laws and the temperature and soil moisture dependence described above, if needed.

432  
 433 **3.4 Plant related processes: root uptake of nitrate as an example**

434 NitrateNutrient uptake by plants is ~~intrinsically~~ complex and remains poorly  
 435 understood (~~Devienne-Barret et al., 2000; Crawford and Glass, 1998; Hachiya and~~  
 436 ~~Sakakibara, 2016~~). A variety of plant uptake models exists with varying degrees of  
 437 complexity (Neitsch et al., 2011; Fisher et al., 2010; Cai et al., 2016). These models are  
 438 mostly based on plant growth module or supply and demand approach that often requires  
 439 detailed phenological and plant attributes ~~such as including~~ growth cycle, root age and  
 440 biomass, nitrate nutrient availability, ~~phosphorous stress~~, and carbon allocation, in  
 441 addition to local ~~climate conditions such as~~ temperature and soil moisture (Neitsch et al.,  
 442 2011; Porporato et al., 2003; Dunbabin et al., 2002; Buysse et al., 1996; Fisher et al., 2010).  
 443 Without detailed ~~information mechanistic understanding~~, we ~~can~~ assume a simple and  
 444 operational approach (~~Eqn. 13 and 14~~). In the Example 2 that we show later, for example,  
 445 ~~we modeled~~ nitrate uptake was modelled with dependence on  $\text{NO}_3^-$  concentration, soil  
 446 temperature and moisture, and rooting density (McMurtrie et al., 2012; Yan et al.,  
 447 2012; Buljovic and Engels, 2001).

$$448 \quad r_{\text{uptake}} = k_{\text{uptake}} C_{\text{NO}_3^-} f(T) f(S_w) f_{\text{root}}(d_w) \quad (13)$$

$$449 \quad f_{\text{root}}(d_w) = \exp((-d_w + \delta) / \lambda) \quad (14)$$

450 Where  $k_{\text{uptake}}$  [L/s] is the nitrate uptake rate,  $f_{\text{root}}(d_w)$  is the normalized rooting density  
 451 term in the range of 0 to 1 as a function of water depth to the groundwater ( $d_w$ ). The  
 452 rooting term (Eqn. 14) was exponentially fitted ( $\delta = 0.013, \lambda = 0.20$ ) based on field  
 453 measurements of root distribution along depth (Hasenmueller et al., 2017). It is common  
 454 to observe root density decrease exponentially in forests (~~López et al., 2004~~) (López et  
 455 al., 2001). Other form of user-tailored plant uptake rate law can be added if needed.

456

#### 457 **4. Numerical scheme and model verification**

458 The system of differential equations for ~~the~~ water storages (e.g., Eqn. 1 and 2, and  
 459 Eqn. S1 and S2) are assembled into a global system of ordinary differential equations  
 460 (ODEs) ~~and solved~~. It issolved in CVODE (short for C-language Variable-coefficients  
 461 ODE solver, <https://computing.llnl.gov/projects/sundials/cvode>), a numerical ODE solver  
 462 in the SUite of Nonlinear and Differential / ALgebraic equation Solvers (SUNDIALS)  
 463 (Hindmarsh et al., 2005). In BioRT, the transport step is first solved with water by the

464 preconditioned Krylov (iterative) method and the Generalized Minimal Residual Method  
465 ~~(Saad and Schultz, 1986)~~(Saad and Schultz, 1986). ~~In the following reaction step, all~~All  
466 primary species in ~~each finite volume~~in element ~~I~~ are ~~then~~ assembled in a local matrix  
467 and ~~then~~ solved iteratively ~~by using~~ the Crank-Nicolson and Newton-Raphson  
468 ~~method~~methods in CVODE (Bao et al., 2017).

469  
470 **Model verification.** The BioRT module had been verified against CrunchTope  
471 under different transport and reaction conditions (Figures S1 – S7 in SI). CrunchTope is  
472 a widely used subsurface reactive transport model (Steefel and Lasaga, 1994;Steefel et  
473 al., 2015), and is often used as a benchmark to verify other reactive transport models.  
474 Verification was performed under simplified hydrological conditions with 1-D column and  
475 constant flow rates such that it focuses on advection, diffusion, dispersion, and  
476 biogeochemical reactions. Specifically, three cases ~~of soil phosphorus, carbon, and~~  
477 ~~nitrogen~~were verified ~~for temporal evolution and spatial pattern of relevant solute~~  
478 ~~concentrations~~. The phosphorus case that involves kinetics-controlled apatite dissolution  
479 and thermodynamics-controlled phosphorous speciation was first tested for solution  
480 accuracy of the bulk code that was inherited from the original RT-Flux-PIHM. Soil carbon  
481 and nitrogen processes ~~that involve microbe-driven processes, such as soil carbon~~  
482 ~~decomposition and mineralization, nitrification and denitrification~~, were further verified for  
483 solution accuracy of the augmented BioRT module. Table S7 shows an average percent  
484 bias and Nash Sutcliffe efficiency (NSE) of 1.1% and 0.98, indicating a robust  
485 performance for a variety of solutes under different transport and reaction conditions.

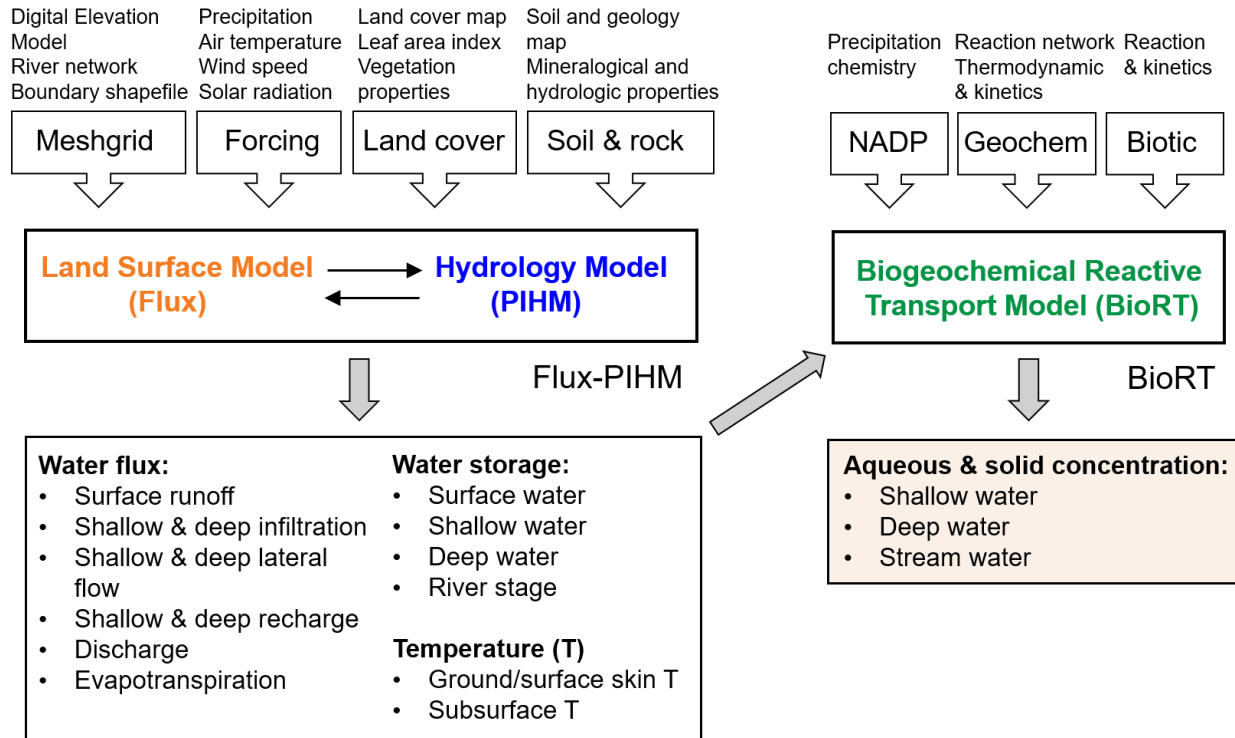
486

## 487 **5. Model structure, data needs, and domain setup**

488 **Model structure.** The model takes meteorological forcing time series as input and  
489 solves for water storages and soil temperature, along with other hydrologic and land  
490 surface states and fluxes (Figure 5). BioRT reads in the model output of water and  
491 temperature from Flux-PIHM, and solves the biogeochemical reactive transport  
492 equations. At the time scale of months to years that are typical for BioRT-Flux-PIHM  
493 simulations, alterations in solid phase properties, including, porosity, permeability, and

494 reactive surface area, are considered negligible such that hydrological parameters remain  
495 constant with time.

496 **Data needs.** The code sets up the model domain based on watershed  
497 characteristics including topography, land cover, and shallow and deep zone properties  
498 (Figure 5). When the model is used in a spatially distributed form, the model domain ~~can~~  
499 ~~be~~ set up using elevation, land cover, soil and geology maps supplied by the user ~~or~~  
500 ~~from the~~. A useful data portal ~~of~~ is the Geospatial Data Gateway  
501 (<https://datagateway.nrcs.usda.gov>). ~~The meteorological~~ Another geospatial data source  
502 is the HydroTerre (<http://www.hydroterre.psu.edu/>), where users can obtain data on  
503 elevation, land cover, geology, and soil (Leonard and Duffy, 2013). ~~Meteorological~~ forcing  
504 data can be downloaded from the North American Land Data Assimilation Systems Phase  
505 2 (NLDAS-2, <https://ldas.gsfc.nasa.gov/nldas/v2/forcing>). The vegetation forcing, i.e.,  
506 Leaf Area Index (LAI), can be obtained from MODIS (Moderate Resolution Imaging  
507 Spectroradiometer, <https://modis.gsfc.nasa.gov/data>). Other vegetation properties  
508 ~~associated with land cover~~ (e.g., shading fraction, rooting depth) can be adopted from,  
509 for example, the Noah vegetation parameter table embedded in the Weather Research  
510 and Forecasting model (WRF; Skamarock and Klemp (2019)). Local measurements from  
511 meteorological stations and field campaigns (e.g., land cover, soil, geology) can ~~also be~~  
512 ~~used in the model.~~ ~~Another data source is the HydroTerre~~  
513 ~~(<http://www.hydroterre.psu.edu/>), where users can obtain geospatial data (e.g., elevation,~~  
514 ~~land cover, geology, soil) (Leonard and Duffy, 2013).~~ be used in the model. Initial water  
515 and solid phase chemistry can be based on measurements or general knowledge of the  
516 simulated sites. The form of reaction rate laws, ~~including the Monod form, temperature~~  
517 ~~and soil moisture dependence,~~ can be defined in the input files and calibrated to  
518 reproduce field data. Reaction thermodynamics, mostly equilibrium constants, are from  
519 the geochemical database EQ3/6 by default (Wolery, 1992). These reaction parameters  
520 can be modified when necessary. The model outputs include aqueous and solid  
521 concentrations of shallow and deep zone and stream water.



522

523 **Figure 5.** Model structure, input, and output of BioRT-Flux-PIHM. The Flux-PIHM takes in  
 524 watershed characteristics including topography (digital elevation model, DEM), land cover,  
 525 shallow and deep zone properties, and meteorological forcing time series and solves for water  
 526 storage, and ground and soil temperature. BioRT takes in water- and temperature-related  
 527 information/output from Flux-PIHM with and additional inputs such as precipitation chemistry and  
 528 shallow and deep water chemistry and biogeochemical kinetics parameters, and solve for  
 529 aqueous and solid concentrations in the shallow and deep zone, and stream water. NADP stands  
 530 for the National Atmospheric Deposition Program. ~~This paper focuses on the BioRT component.~~  
 531 ~~The land surface, hydrological processes, and abiotic reactive transport processes have been~~  
 532 ~~described in previous papers (Bao et al., 2017; Shi et al., 2013). Discussions on how air~~  
 533 ~~temperature and ET influence stream chemistry can be found in Li (2019).~~

534

535 **Domain set up: from simple, spatially lumped to complex, spatially distributed**  
 536 **domains.** The domain can be set up at different spatial resolutions with different numbers  
 537 of grids. A simple domain can be set up with only two land grids representing two sides  
 538 of a watershed connected by one river cell. This setup uses averaged properties without  
 539 needs for larger spatial data. Alternatively, a complex domain can be set up to track “hot  
 540 spots” of biogeochemical reactions using many grids with explicit representation of spatial  
 541 details: (e.g., topographic map, river network, land use map, soil and geology map,  
 542 mineral distribution). The model domain can be set up using PIHM-GIS

543 ([http://www.pihm.psu.edu/pihmgis\\_home.html](http://www.pihm.psu.edu/pihmgis_home.html)), a standalone GIS interface for watershed  
544 delineation, domain decomposition, and parameter assignment (Bhatt et al., 2014). ~~It~~  
545 ~~requires much more data and can be computationally expensive but can be used to~~  
546 ~~identify “hot spots” of biogeochemical reactions within a watershed.~~ The same model  
547 processes (e.g., hydrology, reaction network) can be setup in both types of spatial  
548 configurations. Auto-calibration is not built into the model, but a global calibration  
549 coefficient approach is used to reduce parameter dimension and facilitate manual  
550 calibration. A typical model application requires 20 to 30 hydrological parameters to be  
551 calibrated. These parameters include land surface parameters (e.g., canopy resistance,  
552 surface albedo), soil and geology parameters (e.g., hydraulic conductivity, porosity, Van  
553 Genuchten, macropore properties) (Shi et al., 2013). Reaction-related parameters (e.g.,  
554 reaction rate constant, mineral surface area,  $Q_{10}$ ,  $S_{w,c}$ , and  $n$ ) are additionally needed for  
555 calibration, the number of which depends on the numbers of reactions involved in a  
556 particular system.

557

## 558 **6. Model applications**

559 The original RT-Flux-PIHM has been applied to understand processes related to  
560 the geogenic solutes of Cl and Mg at the Shale Hills watershed and for Na in a watershed  
561 on Volcán Chimborazo in the Ecuadorian Andes (Table 1). The new BioRT-Flux-PIHM  
562 has been demonstrated for understanding the dynamics of DOC and nitrate at Shale Hills  
563 and Coal Creek. This section will present one hydrology and two biogeochemical  
564 examples in the Susquehanna Shale Hills Critical Zone Observatory (SSHCZO), a small  
565 headwater watershed in central Pennsylvania, USA. The mean annual precipitation is  
566 approximately 1,070 mm and the mean annual temperature is 10-°C (Brantley et al.,  
567 2018). Soil carbon storage and respiration and nitrogen budget and fluxes have been  
568 studied in detail (Andrews et al., 2011; Hasenmueller et al., 2015; ~~Shi et al., 2018; Hodges~~  
569 ~~et al., 2019;~~ Weitzman and Kaye, 2018). Modeling work has been conducted to  
570 understand hydrological dynamics (Shi et al., 2013; Xiao et al., 2019), transport of the non-  
571 reactive tracer Cl, and the weathering-derived solute Mg (Bao et al., 2017; Li et al., 2017a).

572 **Table 1.** ~~Existing~~Example Model applications of BioRT-Flux-PIHM

Watershed (location)	Size (km <sup>2</sup> )	Model domain	Modeled solutes	Reactions (rate laws: 1, TST; 2, Monod based; 3, plant uptake)	Reference
Shale Hills (PA, USA)	0.08	Spatially distributed	Cl, Mg	<ul style="list-style-type: none"> <li>Chlorite dissolution<sup>1</sup></li> <li>Illite dissolution<sup>1</sup></li> <li><del>Carbonate dissolution &amp; precipitation<sup>+</sup></del></li> <li>Cation exchange</li> </ul>	Bao et al., 2017; Li et al., 2017
		Spatially distributed	DOC	<ul style="list-style-type: none"> <li>SOC decomposition<sup>2</sup></li> <li>DOC sorption</li> </ul>	Wen et al., 2020
		Spatially lumped	NO <sub>3</sub> <sup>-</sup>	<ul style="list-style-type: none"> <li>Soil N leaching<sup>2</sup></li> <li>Denitrification<sup>2</sup></li> <li>Plant uptake<sup>3</sup></li> </ul>	This work
Coal Creek (CO, USA)	53	Spatially lumped	DOC, Na	<ul style="list-style-type: none"> <li>SOC decomposition<sup>2</sup></li> <li>DOC sorption</li> <li>Albite dissolution<sup>1</sup></li> </ul>	Zhi et al., 2019
Volcán Chimborazo (Ecuador)		Spatially distributed	Cl, Na, Ca, Mg, SiO <sub>2</sub>	<ul style="list-style-type: none"> <li>Albite dissolution<sup>1</sup></li> <li>Diopside dissolution<sup>1</sup></li> </ul>	<del>Saberi et al. (under review)</del> <u>Saberi et al. (2021)</u>

573 Note: Transition State Theory (TST) is a classic kinetic rate law for mineral dissolution and  
574 precipitation (Brantley et al., 2008) (Eqn. ~~S15~~); ~~Monod rate law with environmental dependency~~  
575 ~~(i.e., soil temperature and soil moisture) is widely used for microbially driven reactions. Monod-~~  
576 ~~based and plant nitrate uptake rate law are detailed in the following section of 6.2.S15);~~ SOC  
577 stands for soil organic carbon.

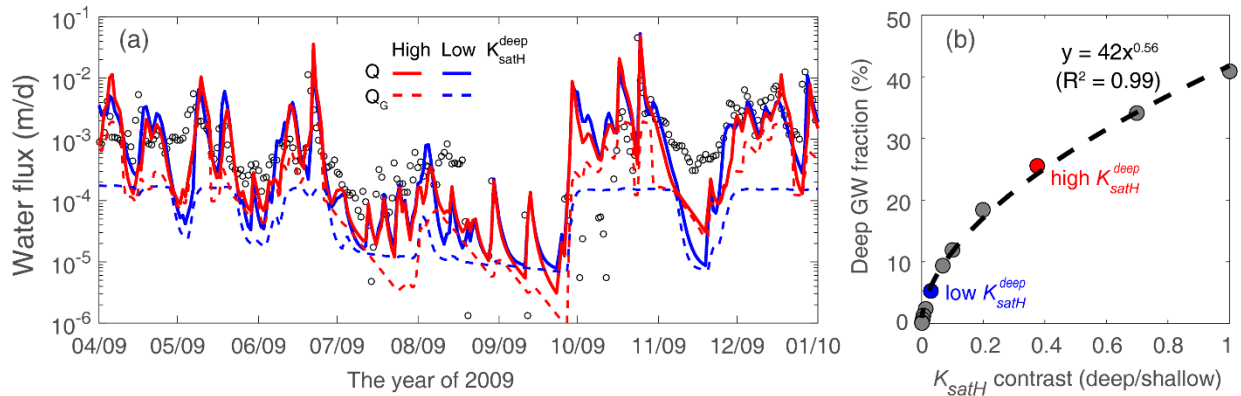
578

## 579 6.1 Example 1: Shallow and deep water interactions

580 The model was set up using the spatially lumped mode with two ~~land~~ grids and  
581 one river grid characterized by average land cover, soil and rock properties based on  
582 previous work ~~(Shi et al., 2013; Kuntz et al., 2011). The model assumed a Weikert soil,~~  
583 ~~the dominant soil type at Shale Hills (Shi et al., 2013).~~ The model assumed the dominant  
584 soil type (Weikert soil) at Shale Hills. The porosity of the deep zone was set to a tenth of  
585 the shallow soil porosity based on measurements of the groundwater aquifer (Brantley et  
586 al., 2018; Kuntz et al., 2011). In a headwater catchment like Shale Hills where the deep  
587 groundwater is most likely sourced from recharge, the deep groundwater contribution to  
588 the stream can be primarily controlled by the hydraulic conductivity ( $K_{satH}$ ) contrast



589 between the deep and shallow zones (i.e.,  $K_{satH}^{dp} / K_{satH}^{sl}$ ). This is because the  $K_{satH}$   
 590 contrast determines the partitioning of infiltrating water between the shallow lateral flow  
 591 and the downward recharge to the deep zone and then deep groundwater flow. Two  
 592 cases of high (red) and low (blue)  $K_{satH}^{dp}$  were set up to showcase the control of  $K_{satH}$   
 593 contrast on deep groundwater (Figure 6a). By changing the deep zone  $K_{satH}^{dp}$  from 2.6 to  
 594 0.22 (m/d), the annual deep groundwater ( $Q_G$ ) contribution to discharge (Q) decreased  
 595 from 26% to 5.2%, although the total stream discharge is negligible, remains the same.  
 596 This indicates that the changing  $K_{satH}^{dp}$  mostly changes the partitioning flow partitioning  
 597 between the shallow soil lateral flow and recharge, whereas total infiltration and discharge  
 598 remain very similar. —deeper groundwater flow into streams.



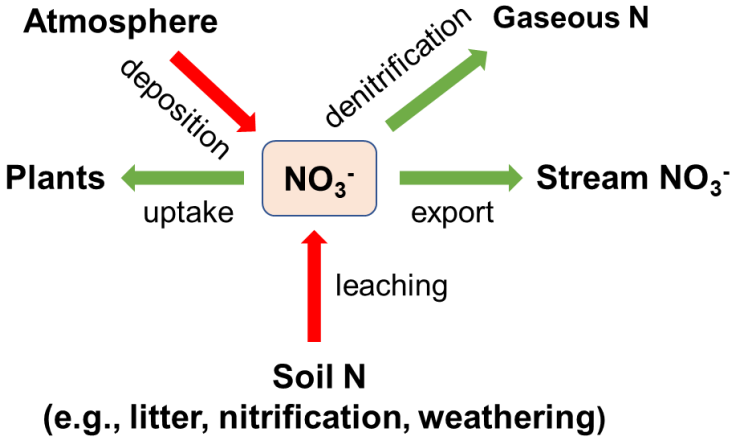
599  
 600 **Figure 6.** (a) Hydraulic conductivity ( $K_{satH}$ ) contrast ~~control on~~ controls the proportion of deep  
 601 groundwater ( $Q_G$ ). The cases of high ( $K_{satH}^{dp} = 2.6$  m/d, red) and low conductivity ( $K_{satH}^{dp} =$   
 602  $0.22$  m/d, blue) led to 26% and 5.2% of annual  $Q_G$  contribution to discharge (Q), respectively. (b)  
 603 Deep groundwater fraction as a function of  $K_{satH}$  contrast between the deep and shallow zone.  
 604 The upper limit of the deep / shallow  $K_{satH}$  contrast was limited set to 1 in the figure as most  
 605 watersheds exhibit a have smaller  $K_{satH}$  in the deep zone than in the shallow zone. The two red  
 606 and blue dots correspond to the two cases in left panel.

607  
 608 Several additional cases were further tested to examine the relationship between  
 609 deep groundwater fraction (%) of discharge and  $K_{satH}$  contrast. Figure 6b shows that the  
 610 deep groundwater fraction rapidly increases with the increasing ratio of  $K_{satH}^{dp} / K_{satH}^{sl}$ ,  
 611 reaching a limit when  $K_{satH}$  contrast is sufficiently high. The deep groundwater  
 612 contribution to the stream reaches ~ 40% when ~~the~~  $K_{satH}^{dp}$  and  $K_{satH}^{sl}$  are equal. In natural

613 systems, we do see places, for example, karst formations, where groundwater contributes  
 614 to more than 40% (~~Hartmann et al., 2014; Husic, 2018~~)([Hartmann et al., 2014; Husic,](#)  
 615 [2018](#)). These places may have higher deeper conductivity than shallow soils due to the  
 616 development of highly conductive conduits.

617  
 618 **6.2 Example 2: Nitrate dynamics in a spatially implicit domain**

619 This example focuses on nitrate ( $\text{NO}_3^-$ ), a dominant dissolved N form in water ~~with~~  
 620 ~~abundant measurements~~ (<https://criticalzone.org/shale-hills/data/datasets/>) (Weitzman  
 621 and Kaye, 2018). The N processes at Shale Hills include atmospheric N deposition, soil  
 622 N leaching, stream export, denitrification, and plant uptake (Figure 7). Based on field  
 623 measurements, the atmospheric deposition at the site is the dominant N input ~~and~~; N  
 624 export via discharge is only a small fraction (2.5%) of atmospheric N input, ~~indicating~~  
 625 ~~most.~~ Most deposited N is tightly cycled by plants or lost to the atmosphere via  
 626 denitrification.



627  
 628 **Figure 7.** Modeled nitrogen processes in Example 2. Atmospheric N deposition is the major N  
 629 input; denitrification and plant uptake are the major N loss and sink. Export via discharge only  
 630 occupies a small fraction.

631  
 632 The soil N leaching process was represented using a lumped reaction that  
 633 generates  $\text{NO}_3^-$ . Conceptually this could represent the total rates of reactions including  
 634 the decomposition of soil organic matter (SOM), nitrification, and rock weathering that  
 635 generates  $\text{NO}_3^-$ . Its rate was assumed to depend on soil temperature and moisture and  
 636 follows the equation  $r_{leach} = kAf(T)f(S_w)$ , where  $r_{leach}$  [mol/s] is the leaching rate,  $k =$

637  $10^{-9.7}$  [mol/m<sup>2</sup>/s] is the leaching rate constant (Regnier and Steefel, 1999), and  $A$  [m<sup>2</sup>] is  
 638 the surface area that represents the contact area between substrates and N transforming  
 639 microbe, and  $f(T)$  and  $f(S_w)$  are soil temperature (Eqn. 8) and soil moisture (Eqn. 9)  
 640 functions, respectively. The surface area was calculated based on SOM volume fraction  
 641 [m<sup>3</sup>/m<sup>3</sup>], specific surface area (SSA, [m<sup>2</sup>/g]), substrate density [g/cm<sup>3</sup>], and element  
 642 volume [m<sup>3</sup>].

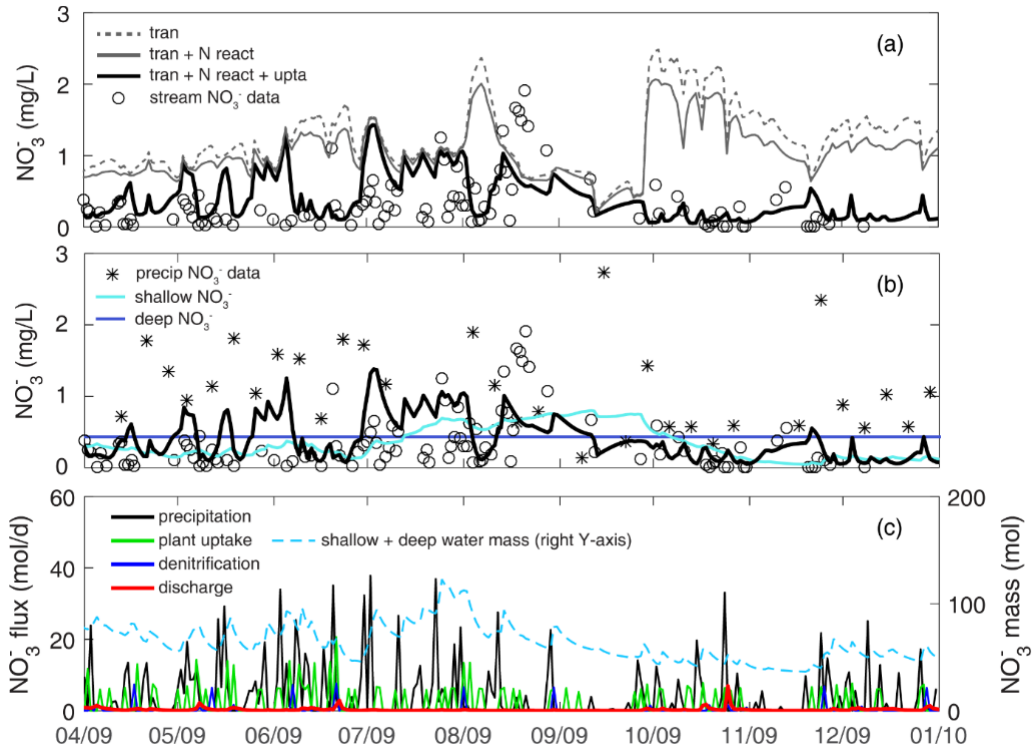
643 Denitrification converts NO<sub>3</sub><sup>-</sup> to N<sub>2</sub> gas under anaerobic conditions. Here this  
 644 process was modeled by the Monod rate law with DOC as the electron donor (Di Capua  
 645 et al., 2019)(Di Capua et al., 2019), NO<sub>3</sub><sup>-</sup> as the electron acceptor, and with an inhibition  
 646 term  $f(O_2)$  (Eqn. S13). The reaction rate:  $r_{denitrification} =$   
 647  $kA \frac{C_{DOC}}{K_{m,DOC} + C_{DOC}} \frac{C_{NO_3^-}}{K_{m,NO_3^-} + C_{NO_3^-}} f(O_2) f(T) f(S_w)$ , where  $k = 10^{-10}$  [mol/m<sup>2</sup>/s] is the  
 648 denitrification rate constant (Regnier and Steefel, 1999), half-saturation constants  
 649  $K_{m,DOC} = 15$  [uM] and  $K_{m,NO_3^-} = 45$  [uM] (Regnier and Steefel, 1999; Billen,  
 650 1977)(Regnier and Steefel, 1999). For soil N leaching and denitrification, the SSA were  
 651 respectively tuned as  $1.6 \times 10^{-6}$  and  $7.5 \times 10^{-5}$  [m<sup>2</sup>/g] to reproduce observed stream nitrate  
 652 dynamics. The calibrated values were orders of magnitude lower than the lab measured  
 653 SSA of natural materials (e.g., SOM, 0.6 ~ 2 m<sup>2</sup>/g) (Rutherford et al., 1992; Chiou et al.,  
 654 1990)(Rutherford et al., 1992). Such discrepancies between calibrated effective reactive  
 655 surface area (i.e., solid-water contact area) and lab measured absolute surface area are  
 656 consistent with other observations in literature (Li et al., 2014; Heidari et al., 2017)(Li et  
 657 al., 2014; Heidari et al., 2017; Wen and Li, 2017, 2018). The uptake rate constant was  
 658 calibrated by constraining the partitioning of N transformation flux between denitrification  
 659 and plant uptake by the ratio of 1:5, a value estimated from field measurements of  
 660 gaseous N outputs (3.53 kg-N/ha/yr) and plant N uptake (18.3 kg-N/ha/yr) (Weitzman and  
 661 Kaye, 2018). ~~The uptake rate constant in the deep zone (> 2 m in depth) was considered~~  
 662 ~~negligible (Weitzman and Kaye, 2018; Hasenmueller et al., 2017)~~ ~~The uptake rate constant~~  
 663 ~~in the deep zone (> 2 m in depth) was considered negligible (Hasenmueller et al., 2017).~~  
 664 Groundwater nitrate was initialized as 0.43 mg/L, the average of measured groundwater  
 665 concentration during 2009 - 2010.

666

667 **Temporal nitrate dynamics.** Three cases were set up to understand and quantify the  
668 effects of different processes in determining nitrate dynamics (Figure 8a). The *transport-*  
669 *only* case (dashed line, *tran*) simulates nitrate input from precipitation (at  $1.4 \pm 0.96$  mg/L,  
670 based on the 2009 data of NADP PA42 site) and N transport but without any reactions. It  
671 overestimated stream nitrate data ( $0.33 \pm 0.39$  mg/L) throughout the year. The *transport*  
672 *+ N reactions* case (gray line, *tran + N react*) has denitrification and soil N leaching  
673 processes but not plant uptake. These two reactions lowered the nitrate concentration  
674 slightly, as these two processes compensate each other in adding and removing nitrate  
675 from water. The *transport + N reactions + uptake* case (thick black line, *tran + N react +*  
676 *upta*) have all processes. It significantly lowered the nitrate concentration, especially in  
677 April-May and October-December. Nitrate peaks from May to July, exhibiting comparable  
678 levels of high ~~precipitation~~-nitrate concentration (Figure 8b). It is noticeable that the three  
679 cases almost overlapped at these overestimated short nitrate peaks, suggesting nitrate-  
680 rich precipitation may not be routed into the subsurface where denitrification and plant  
681 uptake could occur.

682 Although precipitation from April to August accounted for 70% of the total  
683 simulation period, larger storm events in October contributed more to ~~the~~nitrate export.  
684 Deeper groundwater had higher nitrate concentration than shallow water, because most  
685 plant uptake occurred in the shallow zone. The nitrate fluxes into the deeper zone  
686 however only contributed 26% of stream nitrate export at the annual scale, due to the  
687 relatively small groundwater contribution (9.5%) to the stream. Denitrification and plant  
688 uptake largely occurred during ~~the wet spring period, which is part of the leaf-on~~  
689 season with leaves growing. Denitrification peaks often appeared after major storm  
690 events because wet conditions facilitate denitrification. Comparing the three outfluxes  
691 (Figure 8c), nitrate export via discharge (red) was negligible compared to denitrification  
692 (blue) and plant uptake (green). At the annual scale, stream export ~~only~~-accounted for  
693 9.5% outfluxes, %, whereas denitrification and plant uptake took up 15% and 75% of  
694 deposited  $\text{NO}_3^-$ , respectively. In other words, as Nitrate enters this system via  
695 precipitation, plant uptake can play a significant role in reducing nitrate level, indicating  
696 precipitated nitrate is tightly cycled in the system.

697



698

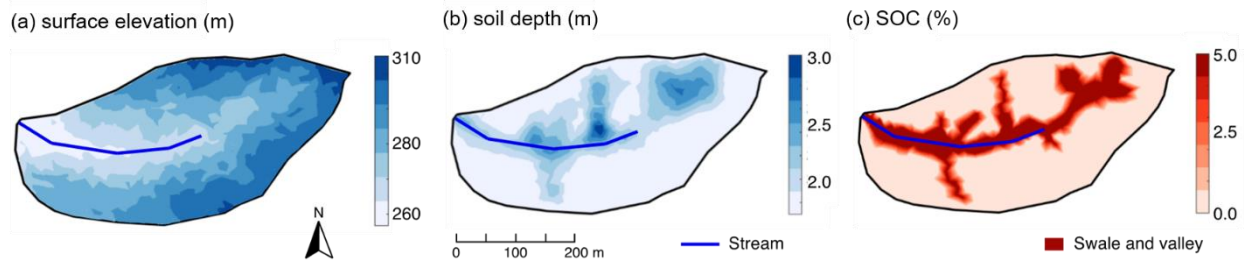
699 **Figure 8.** Stream nitrate dynamics and fluxes at Shale Hills in Example 2. ~~(a) stream nitrate~~  
 700 ~~dynamics in three(a) Three~~ simulation ~~conditionsscenarios~~ with different processes ~~are~~  
 701 ~~demonstrated here:~~ *transport-only* (dashed line, *tran*), *transport + N reaction* (gray line, *tran + N*  
 702 *react*), *transport + N reaction + plant uptake* (thick black line, *tran + N react + upta*), where N  
 703 reactions include both nitrate leaching and denitrification (see Figure 7); (b) nitrate concentration  
 704 in precipitation, shallow and deep water; (c) nitrate fluxes and budget. Note ~~thethat~~ nitrate  
 705 leaching was ignored in (b) due to its minimal flux as ~~precipitation-N~~ deposition from rainfall  
 706 ~~as~~ the dominant input ~~source~~ (Weitzman and Kaye, 2018).

707

### 708 6.3 Example 3: DOC production and export in a spatially distributed domain

709 This example showcases the application of BioRT-Flux-PIHM in a spatially  
 710 distributed mode. This work has been documented with full details in Wen et al. (2020).  
 711 Here we only introduce some key features and capabilities in the spatially distributed  
 712 mode. The Shale Hills catchment was discretized into 535 prismatic land elements and  
 713 20 stream segments through PIHMgis based on the topography (Figure 9a). The  
 714 heterogeneous distributions of soil depth and solid organic carbon within the domain  
 715 (Figure 9b-c) were interpolated through ordinary kriging based on field surveys (Andrews  
 716 et al., 2011; Lin, 2006). Other soil and mineralogy properties such as hydraulic  
 717 conductivity, van Genuchten parameters, and ion exchange capacity were spatially

718 distributed following intensive field measurements (Jin and Brantley, 2011; Jin et al.,  
719 2010; Shi et al., 2013) ([criticalzone.org/shale-hills/data/](http://criticalzone.org/shale-hills/data/)).



720  
721 **Figure 9.** Attributes of Shale Hills in the spatially distributed mode in Example 3: (a) surface  
722 elevation, (b) soil depth, and (c) soil organic carbon (SOC). The surface elevation was generated  
723 from lidar topographic data ([criticalzone.org/shale-hills/data/](http://criticalzone.org/shale-hills/data/)); Soil depths and SOC were  
724 interpolated using ordinary kriging based on field surveys (Andrews et al., 2011; Lin, 2006). The  
725 SOC distribution in (c) was further simplified using the high, uniform SOC (5% v/v) in swales and  
726 valley soils based on field survey (Andrews et al., 2011). Swales and valley floor areas were  
727 defined based on surface elevation via field survey and a 10 m resolution digital elevation model  
728 (Lin, 2006).

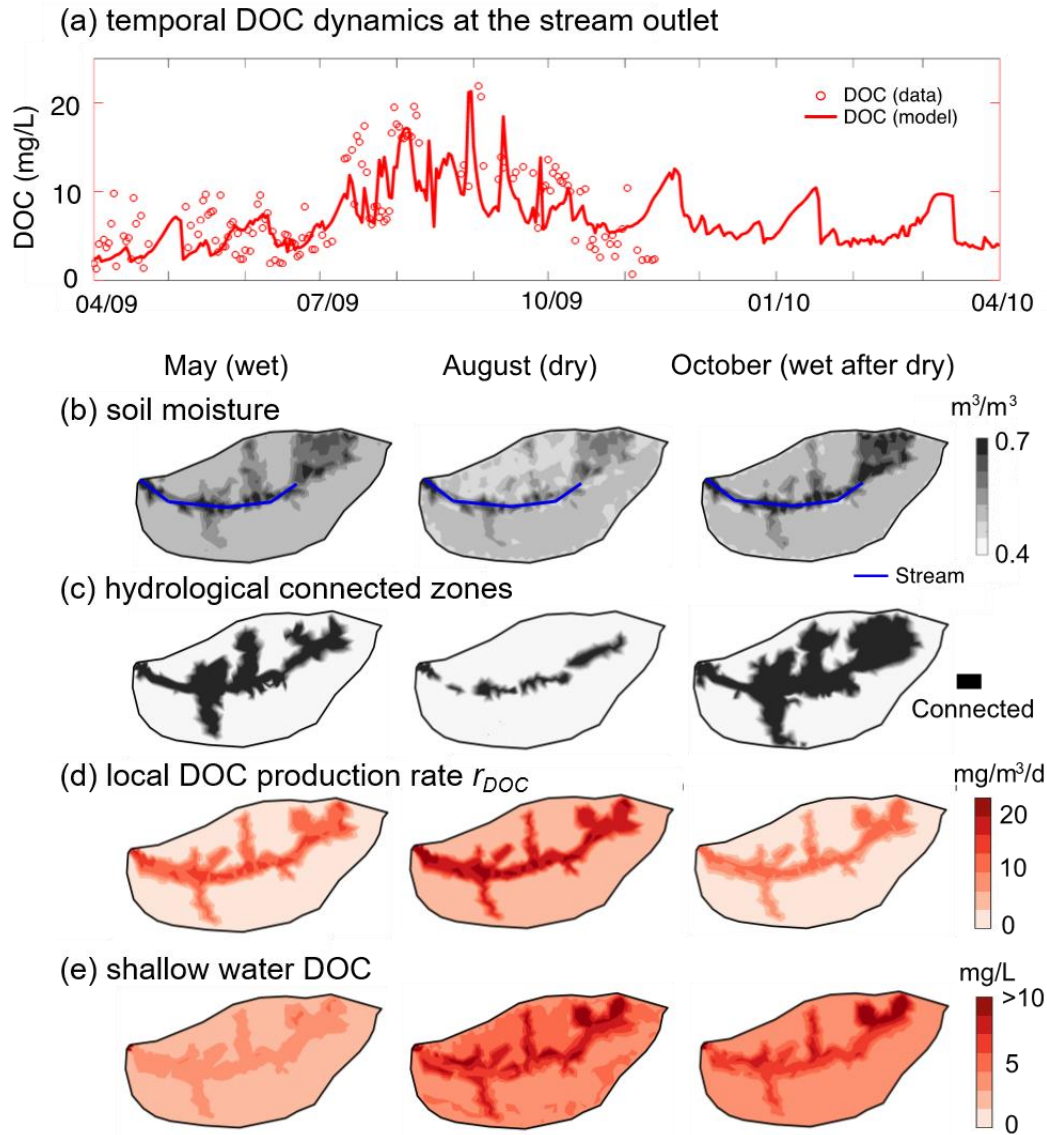
729  
730 **Temporal and spatial patterns of DOC production and export.** The model outputs  
731 followed the general trend of stream DOC measurements ~~(with the model evaluation~~  
732 ~~index~~ NSE = 0.55 for monthly DOC concentration; (Figure 10a), with NSE ranges  
733 from  $-\infty$  to 1.0 (i.e., perfect fit) with values greater than 0.5 considered good performance  
734 for monthly water quality model (Moriassi et al., 2015). The model reproduced high DOC  
735 values (~15 mg/L) in the dry periods (July-September). The model enabled the  
736 identification of ~~spatial patterns and reaction~~ hot spots ~~of reactions~~. In May when soil water  
737 is relatively abundant, the valley and swales with deeper soils (Figure 10b) are generally  
738 ~~tended to be~~ wetter compared to the hillslope and ridgetop, and were hydrologically  
739 connected to the stream (Figure 10b, c). The distribution of local DOC production rate  
740  $r_{DOC}$  and DOC concentration followed that of SOC (Figure 10c) and water content (Figure  
741 10b). Low  $r_{DOC}$  in relatively dry planar hillslopes and uplands resulted in low soil water  
742 DOC. The average stream DOC (~5 mg/L) reflected soil water DOC in the valley and  
743 swales.

744 In August, the hydrologically-connected zones with high water content shrank to  
745 the vicinity of the stream and river bed. With high temperature in summer,  $r_{DOC}$  increased

746 by 2-fold from May across the whole catchment while still exhibited the highest values in  
747 the SOC-rich regions. Soil water DOC concentration increased by a factor of 2 because  
748 the produced DOC was trapped in low soil moisture areas that were not hydrologically  
749 connected to the stream. In the north side with low water content (Figure 10b), the soil  
750 water DOC (~7 mg/L in average) accumulated more than the south side (~5 mg/L in  
751 average). The high shallow water DOC (~10 mg/L) in the stream vicinity dominated the  
752 stream DOC in August.

753 In October, precipitation wetted the catchment again. The hydrologically  
754 connected zones expanded beyond swales and the valley to the upland hillslopes (Figure  
755 10c). The increase in hydrological connectivity zones favored the mixing of shallow water  
756 DOC sourced from upland hillslopes (low DOC), swales, and valley (high DOC) into  
757 stream rather than only from the stream vicinity with high DOC in the dry August, leading  
758 to a drop in stream DOC.

759



760

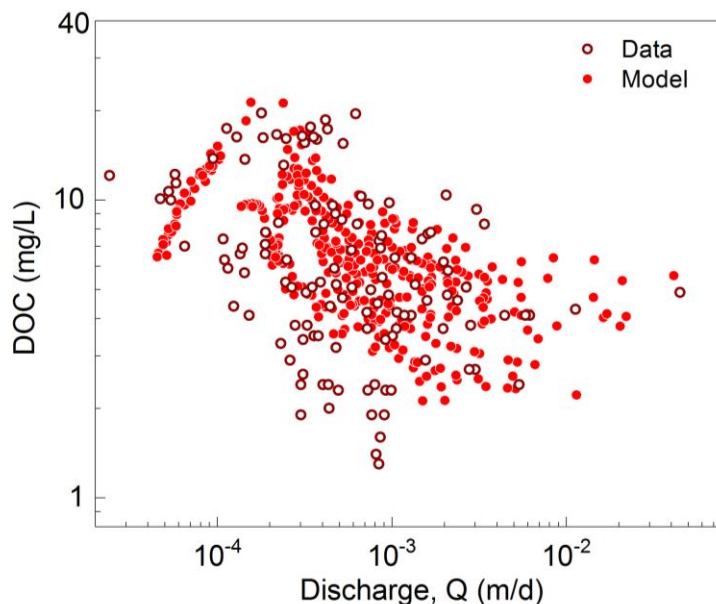
761 **Figure 10.** (a) Temporal dynamics of stream DOC concentration; spatial profiles of (b) shallow  
 762 soil moisture, (c) hydrologically connected zones, (d) local DOC production rates  $r_{DOC}$  and (e)  
 763 shallow water DOC concentration in May (wet), August (dry), and October (wet after dry) of 2009.  
 764 The soil DOC and  $r_{DOC}$  were high in swales and valley with relatively high shallow water and SOC  
 765 content. August had the highest shallow water DOC concentration compared to May and October,  
 766 because most DOC accumulated in zones that are disconnected to the stream.

767

768 **C-Q patterns.** The DOC C-Q relationship showed a non-typical pattern with flushing first  
 769 and transitioning into a dilution pattern, with an overall C-Q slope  $b = -0.23$  (Figure 11).  
 770 At low discharges ( $< 1.8 \times 10^{-4}$  m/d) in the summer dry period, the stream DOC mainly  
 771 came from the organic-rich swales and valley floor zones with high soil water DOC (Figure



772 10e). With discharge increasing in wetter period (i.e., spring and fall), the contribution  
773 from planar hillslopes and uplands with lower DOC concentration increased (Figure 10e),  
774 leading to the dilution of stream DOC.



775  
776 **Figure 11.** Relationships ~~efbetween~~ daily discharge (Q) ~~withand~~ stream DOC concentration. With  
777 the ~~increase-ofincreasing~~ Q, the stream water first shifted from the dominance of groundwater  
778 with low DOC at very low discharge to the predominance of organic-rich soil water from swales  
779 and valley at intermediate discharge. As the discharge increases further, the stream water  
780 switches to the dominance of high flow with lower DOC water from planar hillslopes and uplands,  
781 resulting in a dilution C-Q pattern (modified from Wen et al., 2020).

782  
783 **7. Discussion**

784 ~~The watershed biogeochemical model~~ BioRT-Flux-PIHM brings the reactive  
785 transport modeling capabilities to the watershed scale, enabling the simulation of  
786 subsurface shallow and deep flow paths and biogeochemical reactions influenced by  
787 hydroclimatic conditions and land-surface interactions. The expanded model capability of  
788 simulating bio-mediated processes such as plant uptake, soil respiration, and microbe-  
789 mediated redox reactions enables the simulation of carbon and nutrient cycling in the  
790 shallow subsurface. The inclusion of the deep groundwater zone allows the exploration  
791 of the effects of subsurface structure on hydrological partitioning between shallow soil  
792 lateral flow and deep groundwater, and their relationships with stream discharge.  
793 Although not shown here, the model can also simulate deeper groundwater coming from

794 regional aquifers across the outer boundary. This can be particularly useful for  
795 watersheds of higher stream orders, where a large proportion of deep water may come  
796 from nearby regional aquifers.

797 ~~The model presented here is complex and process-based. The advantage and~~  
798 ~~disadvantages of simple versus complex models have long been debated in the modeling~~  
799 ~~community (Fatichi et al., 2016; Li et al., 2020; Wen et al., 2021).~~ The computational cost  
800 of solving a spatially distributed, nonlinear, multi-component reactive transport model is  
801 high, posing challenges for the application of ensemble-based ~~uncertainty analysis and~~  
802 ~~model weighting/selection methods (Song et al., 2015).~~ ~~With additional reaction analysis.~~  
803 ~~With additional reactions~~ and transport processes, the model includes more functions  
804 (such as reaction kinetic rate laws) and parameters (e.g., reaction rate constants, surface  
805 area) than hydrological models, ~~which have already been criticized for their.~~ ~~The~~  
806 ~~complexity,~~ brings in issues of equifinality, uncertainty, and data demands (Beven, 2001,  
807 2006; Kirchner et al., 1996). These issues will persist even though reactive transport  
808 models will be constrained by additional chemical data. ~~A major source of uncertainty in~~  
809 ~~these models lies in epistemic uncertainties, i.e., the lack of specific knowledge in forcing~~  
810 ~~data and details of reactivities (e.g., spatial distribution and abundance of reactive~~  
811 ~~materials), on top of uncertainties related to hydrology (Beven, 2000; Beven and Freer,~~  
812 ~~2001). The model's conceptual foundations also represent a major source of uncertainty.~~

813 It is in this spirit of “balancing” the cost and gain that we present both spatial  
814 distributed and lumped modes for the BioRT model. (Li et al., 2020). Compared to the  
815 distributed version, the spatially implicit model requires less spatial data, and is  
816 computationally inexpensive, ~~and is relatively easy to set up.~~ It can assess the average  
817 dynamics of ~~the~~ water and solute dynamics and focus on the interactions  
818 among interacting processes without resolving spatial details. The lumped approach can  
819 ~~also~~ accommodate basins with low data availability, and it can be easier for students to  
820 learn ~~to use the model~~. In contrast, spatially explicit representations enable the  
821 exploration of the “hot spots” (e.g., swales and riparian zones with high soil water DOC  
822 concentrations in Figure 10e) and their contribution to stream chemistry at different times.  
823 Spatial heterogeneities in watershed properties (e.g., soil types and depth, lithology,  
824 vegetation, biomass, and mineralogy) are ubiquitous in natural systems. ~~However, a and~~

825 are challenging to resolve. A general understanding of the linkage between local  
826 catchment features and catchment-scale dynamics (e.g., stream concentration dynamics  
827 and solute export pattern) is often lacking. ~~We generally do not understand how spatial~~  
828 ~~heterogeneity affects water flow paths, stream water chemistry, and biogeochemical~~  
829 ~~reaction rates.~~ The spatially distributed model provides a tool to ~~further~~ explore these  
830 questions. Ultimately, the choice of the model complexity level depends on ~~the~~ research  
831 questions that the model is set to answer and the available data. At the end, we all need  
832 to balance cost and gain when deciding to use a simple or complex model, striving to be  
833 “simple but not simplistic” (Beven and Lane, 2019).

834

## 835 **8. Summary and conclusion**

836 This paper introduces the watershed-scale biogeochemical reactive transport code  
837 BioRT (short for BioRT-Flux-PIHM). The code integrates processes of land-surface  
838 interactions, surface hydrology, and multi-component biogeochemical reactive transport.  
839 The new development enables the simulation of 1) biotic reactions including plant uptake,  
840 soil respiration, and microbe-mediated redox reactions, and 2) surface water interactions  
841 with groundwater from deeper subsurface that still interacts with streams. BioRT has been  
842 verified against the widely used reactive transport code CrunchTope for soil carbon,  
843 nitrogen, and phosphorus processes. ~~The BioRT module~~ It has been applied to  
844 understand carbon, nitrogen, and weathering processes in Shale Hills in Pennsylvania,  
845 Coal Creek in Colorado, and Volcán Chimborazo watershed in Andes in Ecuador. Here  
846 we showcase the modeling capability of surface-groundwater interactions and reactive  
847 transport processes relevant to nitrate and DOC in Shale Hills in two simulation modes.  
848 One is in a spatially lumped mode using averaged properties and another is in a spatially  
849 distributed mode with consideration of spatial heterogeneity. Results show that the deep  
850 groundwater flow that interacts with the stream is primarily controlled by the hydraulic  
851 conductivity contrast between shallow and deep zone. biogeochemical reactions in  
852 shallow soil primarily determine the stream water chemistry under high flow conditions.  
853 The spatially lumped method with two lumped grids can capture the temporal dynamics  
854 of average behavior and mass balance; the spatially distributed running mode can be  
855 used to understand the spatial dynamics and to identify “hot spots” of reactions. The code

856 can be used for biogeochemical reactive transport simulations in watersheds under  
857 diverse climate, land cover, and geology conditions.

858  
859 **Data availability.** Field data (e.g., discharge, stream chemistry) is archived at Shale Hills  
860 data portal: <http://criticalzone.org/shale-hills/data/datasets/> or maintained at HydroShare:  
861 <https://www.hydroshare.org/group/147>.

862  
863 **Code availability.** The current model release (BioRT-Flux-PIHM v1.0), ~~including~~  
864 ~~documentation~~ is archived at: <https://doi.org/10.5281/zenodo.3936073>. Documentation,  
865 source code, ~~example data, is and examples are~~ available at GitHub repository:  
866 <https://github.com/PSUmodeling/BioRT-Flux-PIHM>. [https://github.com/Li-Reactive-](https://github.com/Li-Reactive-Water-Group/BioRT-Flux-PIHM)  
867 [Water-Group/BioRT-Flux-PIHM](https://github.com/Li-Reactive-Water-Group/BioRT-Flux-PIHM).

868  
869 **Competing interests.** The authors declare that they have no conflict of interest.

870  
871 **Author contributions.** LL conceived the model idea and oversaw the model  
872 development. WZ coded the BioRT module, verified the code against the benchmark  
873 reactive transport model CrunchTope, and applied and tested the model at Shale Hills  
874 watershed. YS developed the deep groundwater component and integrated the BioRT-  
875 Flux-PIHM v1.0 into the MM-PIHM family. WH, LS, KS, DK, BS, and GHCN tested the  
876 code during its development and contributed study cases.

877  
878 **Acknowledgement.** We acknowledge the funding support from the Department of  
879 Energy, Subsurface Biogeochemistry Program DE-SC0020146, National Science  
880 Foundation Hydrological Sciences EAR-1758795. LS and GCN were supported by  
881 National Science Foundation Grant EAR-1759071. We appreciate data from the  
882 Susquehanna Shale Hills Critical Zone Observatory (SSHCZO) supported by National  
883 Science Foundation Grant EAR – 0725019 (C. Duffy), EAR – 1239285 (S. Brantley), and  
884 EAR – 1331726 (S. Brantley). Data were collected in Penn State's Stone Valley Forest,  
885 which is funded by the Penn State College of Agriculture Sciences, Department of

886 Ecosystem Science and Management, and managed by the staff of the Forestlands  
887 Management Office.

## 888 References

- 889 Andrews, D. M., Lin, H., Zhu, Q., Jin, L., and Brantley, S. L.: Hot spots and hot moments of dissolved organic  
890 carbon export and soil organic carbon storage in the Shale Hills catchment, Vadose Zone Journal, 10, 943-  
891 954, 2011.
- 892 ~~Anyah, R. O., Weaver, C. P., Miguez - Macho, G., Fan, Y., and Robock, A.: Incorporating water table  
893 dynamics in climate modeling: 3. Simulated groundwater influence on coupled land - atmosphere  
894 variability, Journal of Geophysical Research: Atmospheres, 113, 2008.~~
- 895 Bai, J., Zhang, G., Zhao, Q., Lu, Q., Jia, J., Cui, B., and Liu, X.: Depth-distribution patterns and control of soil  
896 organic carbon in coastal salt marshes with different plant covers, Sci Rep-Uk, 6, 34835,  
897 10.1038/srep34835, 2016.
- 898 Bailey, R., Rathjens, H., Bieger, K., Chaubey, I., and Arnold, J.: SWATMOD-Prep: Graphical User Interface  
899 for Preparing Coupled SWAT-MODFLOW Simulations, JAWRA Journal of the American Water Resources  
900 Association, 53, 400-410, <https://doi.org/10.1111/1752-1688.12502>, 2017.
- 901 Bao, C., Wu, H., Li, L., Newcomer, D., Long, P. E., and Williams, K. H.: Uranium Bioreduction Rates across  
902 Scales: Biogeochemical Hot Moments and Hot Spots during a Biostimulation Experiment at Rifle, Colorado,  
903 Environmental Science & Technology, 48, 10116-10127, 10.1021/es501060d, 2014.
- 904 Bao, C., Li, L., Shi, Y., and Duffy, C.: Understanding watershed hydrogeochemistry: 1. Development of RT -  
905 Flux - PIHM, Water Resources Research, 53, 2328-2345, 2017.
- 906 Basu, N. B., Destouni, G., Jawitz, J. W., Thompson, S. E., Loukinova, N. V., Darracq, A., Zanardo, S., Yaeger,  
907 M., Sivapalan, M., Rinaldo, A., and Rao, P. S. C.: Nutrient loads exported from managed catchments reveal  
908 emergent biogeochemical stationarity, Geophys. Res. Lett., 37, 10.1029/2010GL045168, 2010.
- 909 ~~Benettin, P., Fovet, O., and Li, L.: Nitrate removal and young stream water fractions at the catchment  
910 scale, Hydrological Processes, 34, 2725-2738, <https://doi.org/10.1002/hyp.13781>, 2020.~~
- 911 Beven, K.: How far can we go in distributed hydrological modelling?, Hydrol. Earth Syst. Sci., 5, 1-12,  
912 10.5194/hess-5-1-2001, 2001.
- 913 ~~Beven, K., and Freer, J.: Equifinality, data assimilation, and uncertainty estimation in mechanistic  
914 modelling of complex environmental systems using the GLUE methodology, Journal of Hydrology, 249,  
915 11-29, 10.1016/S0022-1694(01)00421-8, 2001.~~
- 916 ~~Beven, K.: A manifesto for the equifinality thesis, Journal of Hydrology, 320, 18-36,  
917 10.1016/j.jhydrol.2005.07.007, 2006.~~
- 918 Beven, K., and Lane, S.: Invalidation of Models and Fitness-for-Purpose: A Rejectionist Approach, in:  
919 Computer Simulation Validation: Fundamental Concepts, Methodological Frameworks, and Philosophical  
920 Perspectives, edited by: Beisbart, C., and Saam, N. J., Springer International Publishing, Cham, 145-171,  
921 2019.
- 922 ~~Beven, K. J.: Uniqueness of place and process representations in hydrological modelling, Hydrol. Earth  
923 Syst. Sci., 4, 203-213, 10.5194/hess-4-203-2000, 2000.~~
- 924 Bhatt, G., Kumar, M., and Duffy, C. J.: A tightly coupled GIS and distributed hydrologic modeling  
925 framework, Environmental Modelling & Software, 62, 70-84,  
926 <http://dx.doi.org/10.1016/j.envsoft.2014.08.003>, 2014.
- 927 ~~Billen, G.: Etude écologique des transformations de l'azote dans les sédiments marins, 1977.~~
- 928 ~~Botter, M., Li, L., Hartmann, J., Burlando, P., and Fatichi, S.: Depth of Solute Generation Is a Dominant  
929 Control on Concentration-Discharge Relations, Water Resources Research, 56, e2019WR026695,  
930 <https://doi.org/10.1029/2019WR026695>, 2020.~~
- 931 Bracho, R., Natali, S., Pegoraro, E., Crummer, K. G., Schädel, C., Celis, G., Hale, L., Wu, L., Yin, H., and Tiedje,  
932 J. M.: Temperature sensitivity of organic matter decomposition of permafrost-region soils during  
933 laboratory incubations, Soil Biology and Biochemistry, 97, 1-14, 2016.
- 934 Brantley, S. L., Kubicki, J. D., and White, A. F.: Kinetics of water-rock interaction, 2008.

935 Brantley, S. L., White, T., West, N., Williams, J. Z., Forsythe, B., Shapich, D., Kaye, J., Lin, H., Shi, Y. N., Kaye,  
936 M., Herndon, E., Davis, K. J., He, Y., Eissenstat, D., Weitzman, J., DiBiase, R., Li, L., Reed, W., Brubaker, K.,  
937 and Gu, X.: Susquehanna Shale Hills Critical Zone Observatory: Shale Hills in the Context of Shaver's Creek  
938 Watershed, *Vadose Zone Journal*, 17, 1-19, ARTN 180092  
939 10.2136/vzj2018.04.0092, 2018.

~~940 Brooks, P. D., Chorover, J., Fan, Y., Godsey, S. E., Maxwell, R. M., McNamara, J. P., and Tague, C.:  
941 Hydrological partitioning in the critical zone: Recent advances and opportunities for developing  
942 transferable understanding of water cycle dynamics, *Water Resources Research*, 51, 6973-6987,  
943 <https://doi.org/10.1002/2015WR017039>, 2015.~~

944 Buljovic, Z., and Engels, C.: Nitrate uptake ability by maize roots during and after drought stress, *Plant  
945 and Soil*, 229, 125-135, 2001.

946 Buysse, J., Smolders, E., and Merckx, R.: Modelling the uptake of nitrate by a growing plant with an  
947 adjustable root nitrate uptake capacity, *Plant and Soil*, 181, 19-23, 1996.

948 Cai, X., Yang, Z.-L., Fisher, J., Zhang, X., Barlage, M., and Chen, F.: Integration of nitrogen dynamics into  
949 the Noah-MP land surface model v1. 1 for climate and environmental predictions, *Geoscientific Model  
950 Development (Online)*, 9, 2016.

~~951 Chiou, C. T., Lee, J. F., and Boyd, S. A.: The surface area of soil organic matter, *Environmental Science &  
952 Technology*, 24, 1164-1166, 1990.~~

~~953 Condon, L. E., Maxwell, R. M., and Gangopadhyay, S.: The impact of subsurface conceptualization on land  
954 energy fluxes, *Advances in Water Resources*, 60, 188-203,  
955 <https://doi.org/10.1016/j.advwatres.2013.08.001>, 2013.~~

~~956 Crawford, N. M., and Glass, A. D.: Molecular and physiological aspects of nitrate uptake in plants, *Trends  
957 in plant science*, 3, 389-395, 1998.~~

958 Davidson, E. A., and Janssens, I. A.: Temperature sensitivity of soil carbon decomposition and feedbacks  
959 to climate change, *Nature*, 440, 165-173, 10.1038/nature04514, 2006.

960 Davidson, E. A., Janssens, I. A., and Luo, Y.: On the variability of respiration in terrestrial ecosystems:  
961 moving beyond Q10, *Global Change Biology*, 12, 154-164, 2006.

962 Davidson, E. A., Janssens, I.A.: Temperature sensitivity of soil carbon decomposition and feedbacks to  
963 climate change, *Nature*, 440, 165-173, 2006.

~~964 Devienne-Barret, F., Justes, E., Machel, J., and Mary, B.: Integrated control of nitrate uptake by crop  
965 growth rate and soil nitrate availability under field conditions, *Annals of Botany*, 86, 995-1005, 2000.~~

966 Di Capua, F., Pirozzi, F., Lens, P. N. L., and Esposito, G.: Electron donors for autotrophic denitrification,  
967 *Chemical Engineering Journal*, 362, 922-937, <https://doi.org/10.1016/j.cej.2019.01.069>, 2019.

968 Dingman, S. L.: *Physical hydrology*, Waveland press, 2015.

969 Dunbabin, V. M., Diggle, A. J., Rengel, Z., and Van Hugten, R.: Modelling the interactions between water  
970 and nutrient uptake and root growth, *Plant and Soil*, 239, 19-38, 2002.

~~971 Edwards, P. J., Williard, K. W. J., and Schoonover, J. E.: Fundamentals of Watershed Hydrology, *Journal of  
972 Contemporary Water Research & Education*, 154, 3-20, 10.1111/j.1936-704X.2015.03185.x, 2015.~~

973 Fatichi, S., Vivoni, E. R., Ogden, F. L., Ivanov, V. Y., Mirus, B., Gochis, D., Downer, C. W., Camporese, M.,  
974 Davison, J. H., ~~Ebel, B., Jones, N., Kim, J., Mascaro, G., Niswonger, R., Restrepo, P., Rigon, R., Shen, C., Sulis,  
975 M., and Tarboton, D.~~ ~~Ebel, B.:~~ An overview of current applications, challenges, and future trends in  
976 distributed process-based models in hydrology, *Journal of Hydrology*, 537, 45-60,  
977 <https://doi.org/10.1016/j.jhydrol.2016.03.026>, 2016-2016.

978 Fatichi, S., Manzoni, S., Or, D., and Paschalis, A.: A Mechanistic Model of Microbially Mediated Soil  
979 Biogeochemical Processes: A Reality Check, *Global Biogeochemical Cycles*, 33, 620-648,  
980 10.1029/2018gb006077, 2019.

981 Fisher, J., Sitch, S., Malhi, Y., Fisher, R., Huntingford, C., and Tan, S. Y.: Carbon cost of plant nitrogen  
982 acquisition: A mechanistic, globally applicable model of plant nitrogen uptake, retranslocation, and  
983 fixation, *Global Biogeochemical Cycles*, 24, 2010.

984 Friedlingstein, P., Cox, P., Betts, R., Bopp, L., von Bloh, W., Brovkin, V., Cadule, P., Doney, S., Eby, M., and  
985 Fung, I.: Climate–carbon cycle feedback analysis: results from the C4MIP model intercomparison, *Journal*  
986 *of climate*, 19, 3337–3353, 2006.

987 ~~Gassman, P. W., Reyes, M. R., Green, C. H., and Arnold, J. G.: The soil and water assessment tool: Historical~~  
988 ~~development, applications, and future research directions, *T Asabe*, 50, 1211–1250, 2007.~~

989 Gatel, L., Lauvernet, C., Carluer, N., Weill, S., Tournebize, J., and Paniconi, C.: Global evaluation and  
990 sensitivity analysis of a physically based flow and reactive transport model on a laboratory experiment,  
991 *Environmental Modelling & Software*, 113, 73–83, <https://doi.org/10.1016/j.envsoft.2018.12.006>, 2019.

992 ~~Gleeson, T., Befus, K. M., Jasechko, S., Luijendijk, E., and Cardenas, M. B.: The global volume and~~  
993 ~~distribution of modern groundwater, *Nature Geoscience*, 9, 161, 10.1038/ngeo2590~~

994 ~~<https://www.nature.com/articles/ngeo2590#supplementary-information>, 2015.~~

995 Godsey, S. E., Kirchner, J. W., and Clow, D. W.: Concentration–discharge relationships reflect chemostatic  
996 characteristics of US catchments, *Hydrol. Process.*, 23, 1844–1864, 10.1002/hyp.7315, 2009.

997 Godsey, S. E., Hartmann, J., and Kirchner, J. W.: Catchment chemostasis revisited: Water quality responds  
998 differently to variations in weather and climate, *Hydrological Processes*, 33, 3056–3069,  
999 <https://doi.org/10.1002/hyp.13554>, 2019.

1000 Grathwohl, P., Rügner, H., Wöhling, T., Osenbrück, K., Schwientek, M., Gayler, S., Wollschläger, U., Selle,  
1001 B., Pause, M., and Delfs, J.-O.: Catchments as reactors: a comprehensive approach for water fluxes and  
1002 solute turnover, *Environmental earth sciences*, 69, 317–333, 2013.

1003 Green, T. R.: Linking climate change and groundwater, in: *Integrated groundwater management*, Springer,  
1004 Cham, 97–141, 2016.

1005 Gurdak, J. J.: Groundwater: Climate-induced pumping, *Nature Geoscience*, 10, 71, 2017.

1006 ~~Hachiya, T., and Sakakibara, H.: Interactions between nitrate and ammonium in their uptake, allocation,~~  
1007 ~~assimilation, and signaling in plants, *Journal of Experimental Botany*, 68, 2501–2512, 10.1093/jxb/erw449,~~  
1008 ~~2016.~~

1009 Hamamoto, S., Moldrup, P., Kawamoto, K., and Komatsu, T.: Excluded - volume expansion of Archie's law  
1010 for gas and solute diffusivities and electrical and thermal conductivities in variably saturated porous  
1011 media, *Water Resources Research*, 46, 2010.

1012 Han, B., Benner, S. G., and Flores, A. N.: Including Variability across Climate Change Projections in  
1013 Assessing Impacts on Water Resources in an Intensively Managed Landscape, *Water*, 11, 286, 2019.

1014 Hararuk, O., Smith, M. J., and Luo, Y.: Microbial models with data-driven parameters predict stronger soil  
1015 carbon responses to climate change, *Glob. Chang. Biol.*, 21, 2439–2453, 10.1111/gcb.12827, 2015.

1016 HARTLEY, I. P., HEINEMEYER, A., and INESON, P.: Effects of three years of soil warming and shading on the  
1017 rate of soil respiration: substrate availability and not thermal acclimation mediates observed response,  
1018 *Global Change Biology*, 13, 1761–1770, <https://doi.org/10.1111/j.1365-2486.2007.01373.x>, 2007.

1019 Hartmann, J., Lauerwald, R., and Moosdorf, N.: A brief overview of the GLObal River CHEmistry Database,  
1020 *GLORICH, Procedia Earth and Planetary Science*, 10, 23–27, 2014.

1021 Hasenmueller, E. A., Jin, L., Stinchcomb, G. E., Lin, H., Brantley, S. L., and Kaye, J. P.: Topographic controls  
1022 on the depth distribution of soil CO<sub>2</sub> in a small temperate watershed, *Applied Geochemistry*, 63, 58–69,  
1023 2015.

1024 Hasenmueller, E. A., Gu, X., Weitzman, J. N., Adams, T. S., Stinchcomb, G. E., Eissenstat, D. M., Drohan, P.  
1025 J., Brantley, S. L., and Kaye, J. P.: Weathering of rock to regolith: The activity of deep roots in bedrock  
1026 fractures, *Geoderma*, 300, 11–31, 2017.



1027 Heidari, P., Li, L., Jin, L., Williams, J. Z., and Brantley, S. L.: A reactive transport model for Marcellus shale  
1028 weathering, *Geochimica et Cosmochimica Acta*, 217, 421-440, 2017.

1029 Herndon, E. M., Dere, A. L., Sullivan, P. L., Norris, D., Reynolds, B., and Brantley, S. L.: Landscape  
1030 heterogeneity drives contrasting concentration–discharge relationships in shale headwater catchments,  
1031 *Hydrology and earth system sciences*, 19, 3333-3347, 2015.

1032 Hindmarsh, A. C., Brown, P. N., Grant, K. E., Lee, S. L., Serban, R., Shumaker, D. E., and Woodward, C. S.:  
1033 SUNDIALS: Suite of nonlinear and differential/algebraic equation solvers, *ACM Transactions on*  
1034 *Mathematical Software (TOMS)*, 31, 363-396, 2005.

~~1035 Hodges, C., Kim, H., Brantley, S. L., and Kaye, J.: Soil CO<sub>2</sub> and O<sub>2</sub> Concentrations Illuminate the Relative  
1036 Importance of Weathering and Respiration to Seasonal Soil Gas Fluctuations, *Soil Science Society of  
1037 America Journal*, 83, 1167-1180, 2019.~~

1038 Hubbard, S. S., Williams, K. H., Agarwal, D., Banfield, J., Beller, H., Bouskill, N., Brodie, E., Carroll, R.,  
1039 Dafflon, B., and Dwivedi, D.: The East River, Colorado, Watershed: A mountainous community testbed for  
1040 improving predictive understanding of multiscale hydrological–biogeochemical dynamics, *Vadose Zone  
1041 Journal*, 17, 2018.

1042 Husic, A.: Numerical modeling and isotope tracers to investigate karst biogeochemistry and transport  
1043 processes, 2018.

1044 Jin, L., and Brantley, S. L.: Soil chemistry and shale weathering on a hillslope influenced by convergent  
1045 hydrologic flow regime at the Susquehanna/Shale Hills Critical Zone Observatory, *Applied Geochemistry*,  
1046 26, Supplement, S51-S56, <http://dx.doi.org/10.1016/j.apgeochem.2011.03.027>, 2011.

1047 Jin, L. X., Ravella, R., Ketchum, B., Bierman, P. R., Heaney, P., White, T., and Brantley, S. L.: Mineral  
1048 weathering and elemental transport during hillslope evolution at the Susquehanna/Shale Hills Critical  
1049 Zone Observatory, *Geochim Cosmochim Acta*, 74, 3669-3691, [10.1016/j.gca.2010.03.036](https://doi.org/10.1016/j.gca.2010.03.036), 2010.

1050 Keune, J., Gasper, F., Goergen, K., Hense, A., Shrestha, P., Sulis, M., and Kollet, S.: Studying the influence  
1051 of groundwater representations on land surface-atmosphere feedbacks during the European heat wave  
1052 in 2003, *Journal of Geophysical Research: Atmospheres*, 121, 13,301-313,325,  
1053 <https://doi.org/10.1002/2016JD025426>, 2016.

1054 Kirchner, J. W., Hooper, R. P., Kendall, C., Neal, C., and Leavesley, G.: Testing and validating environmental  
1055 models, *Science of the Total Environment*, 183, 33-47, [10.1016/0048-9697\(95\)04971-1](https://doi.org/10.1016/0048-9697(95)04971-1), 1996.

~~1056 Kirchner, J. W.: A double paradox in catchment hydrology and geochemistry, *Hydrol. Process.*, 17, 871–  
1057 874, [10.1002/hyp.5108](https://doi.org/10.1002/hyp.5108), 2003.~~

1058 Kuntz, B. W., Rubin, S., Berkowitz, B., and Singha, K.: Quantifying Solute Transport at the Shale Hills Critical  
1059 Zone Observatory, *Vadose Zone Journal*, 10, 843-857, [10.2136/vzj2010.0130](https://doi.org/10.2136/vzj2010.0130), 2011.

~~1060 Lam, Q. D., Schmalz, B., and Fohrer, N.: Modelling point and diffuse source pollution of nitrate in a rural  
1061 lowland catchment using the SWAT model, *Agricultural Water Management*, 97, 317-325,  
1062 <https://doi.org/10.1016/j.agwat.2009.10.004>, 2010.~~

1063 Leonard, L., and Duffy, C. J.: Essential terrestrial variable data workflows for distributed water resources  
1064 modeling, *Environmental modelling & software*, 50, 85-96, 2013.

1065 Li, L., Salehikhoo, F., Brantley, S. L., and Heidari, P.: Spatial zonation limits magnesite dissolution in porous  
1066 media, *Geochimica et Cosmochimica Acta*, 126, 555-573, [10.1016/j.gca.2013.10.051](https://doi.org/10.1016/j.gca.2013.10.051), 2014.

1067 Li, L., Bao, C., Sullivan, P. L., Brantley, S., Shi, Y., and Duffy, C.: Understanding watershed  
1068 hydrogeochemistry: 2. Synchronized hydrological and geochemical processes drive stream chemostatic  
1069 behavior, *Water Resources Research*, 53, 2346-2367, 2017a.

1070 Li, L., Maher, K., Navarre-Sitchler, A., Druhan, J., Meile, C., Lawrence, C., Moore, J., Perdrial, J., Sullivan, P.,  
1071 Thompson, A., Jin, L., Bolton, E. W., Brantley, S. L., Dietrich, W. E., Mayer, K. U., Steefel, C. I., Valocchi, A.,  
1072 Zachara, J., Kocar, B., McIntosh, J., Tutolo, B. M., Kumar, M., Sonnenthal, E., Bao, C., and Beisman, J.:  
1073 Expanding the role of reactive transport models in critical zone processes, *Earth-Science Reviews*, 165,  
1074 280-301, <http://dx.doi.org/10.1016/j.earscirev.2016.09.001>, 2017b.

1075 Li, L.: Watershed reactive transport, *Reviews in Mineralogy and Geochemistry*, 85, 381-418, 2019.

1076 Li, L., Sullivan, P. L., Benettin, P., Cirpka, O. A., Bishop, K., Brantley, S. L., Knapp, J. L. A., Meerveld, I.,  
1077 Rinaldo, A., Seibert, J., Wen, H., and Kirchner, J. W.: Toward catchment hydro - biogeochemical theories,  
1078 *WIREs Water*, 10.1002/wat2.1495, 2020.

1079 Lin, H.: Temporal stability of soil moisture spatial pattern and subsurface preferential flow pathways in  
1080 the ~~shale hills catchment~~*Shale Hills Catchment*, *Vadose Zone Journal*, 5, 317-340, ~~10.2136/vzj2005.0058~~,  
1081 2006.

1082 Lindström, G., Rosberg, J., and Arheimer, B.: Parameter Precision in the HBV-NP Model and Impacts on  
1083 Nitrogen Scenario Simulations in the Rönneå River, Southern Sweden, *AMBIO: A Journal of the Human*  
1084 *Environment*, 34, 533-537, 535, 2005.

1085 Lindström, G., Pers, C., Rosberg, J., Strömqvist, J., and Arheimer, B.: Development and testing of the HYPE  
1086 (Hydrological Predictions for the Environment) water quality model for different spatial scales, *Hydrology*  
1087 *Research*, 41, 295-319, 10.2166/nh.2010.007, 2010.

1088 Liu, Y., Wang, C., He, N., Wen, X., Gao, Y., Li, S., Niu, S., Butterbach - Bahl, K., Luo, Y., and Yu, G.: A global  
1089 synthesis of the rate and temperature sensitivity of soil nitrogen mineralization: latitudinal patterns and  
1090 mechanisms, *Global change biology*, 23, 455-464, 2017.

1091 ~~Lloyd, J., and Taylor, J. A.: On the Temperature Dependence of Soil Respiration, *Functional Ecology*, 8, 315-~~  
1092 ~~323, 10.2307/2389824, 1994.~~

1093 López, B., Sabaté, S., and Gracia, C.: Vertical distribution of fine root density, length density, area index  
1094 and mean diameter in a *Quercus ilex* forest, *Tree Physiology*, 21, 555-560, 2001.

1095 ~~Maavara, T., Lauerwald, R., Laruelle, G. G., Akbarzadeh, Z., Bouskill, N. J., Van Cappellen, P., and Regnier,~~  
1096 ~~P.: Nitrous oxide emissions from inland waters: Are IPCC estimates too high?, *Global Change Biology*, 0,~~  
1097 ~~doi:10.1111/gcb.14504, 2018.~~

1098 ~~Martínez-de la Torre, A., and Miguez-Macho, G.: Groundwater influence on soil moisture memory and~~  
1099 ~~land-atmosphere fluxes in the Iberian Peninsula, *Hydrology and Earth System Sciences*, 23, 4909-4932,~~  
1100 ~~2019.~~

1101 ~~Maxwell, R. M., Lundquist, J. K., Mirocha, J. D., Smith, S. G., Woodward, C. S., and Tompson, A. F.:~~  
1102 ~~Development of a coupled groundwater-atmosphere model, *Monthly Weather Review*, 139, 96-116,~~  
1103 ~~2011.~~

1104 ~~Mayer, K. U., Frind, E. O., and Blowes, D. W.: Multicomponent reactive transport modeling in variably~~  
1105 ~~saturated porous media using a generalized formulation for kinetically controlled reactions, *Water*  
1106 ~~Resources Research, 38, 13-11-13-21, 10.1029/2001wr000862, 2002.~~~~

1107 McMurtrie, R. E., Iversen, C. M., Dewar, R. C., Medlyn, B. E., Näsholm, T., Pepper, D. A., and Norby, R. J.:  
1108 Plant root distributions and nitrogen uptake predicted by a hypothesis of optimal root foraging, *Ecology*  
1109 *and Evolution*, 2, 1235-1250, 2012.

1110 Miller, M. P., Tesoriero, A. J., Hood, K., Terziotti, S., and Wolock, D. M.: Estimating Discharge and Nonpoint  
1111 Source Nitrate Loading to Streams From Three End-Member Pathways Using High-Frequency Water  
1112 Quality Data, *Water Resources Research*, 53, 10201-10216, 10.1002/2017wr021654, 2017.

1113 Miller, M. P., Capel, P. D., García, A. M., and Ator, S. W.: Response of Nitrogen Loading to the Chesapeake  
1114 Bay to Source Reduction and Land Use Change Scenarios: A SPARROW - Informed Analysis, *JAWRA*  
1115 *Journal of the American Water Resources Association*, 56, 100-112, 2020.

1116 Moatar, F., Abbott, B. W., Minaudo, C., Curie, F., and Pinay, G.: Elemental properties, hydrology, and  
1117 biology interact to shape concentration - discharge curves for carbon, nutrients, sediment, and major  
1118 ions, *Water Resources Research*, 53, 1270-1287, 2017.

1119 ~~Moriasi, D. N., Gewda, P. H., Arnold, J. G., Mulla, D. J., Ale, S., and Steiner, J. L.: Modeling the impact of~~  
1120 ~~nitrogen fertilizer application and tile drain configuration on nitrate leaching using SWAT, *Agricultural*  
1121 ~~Water Management, 130, 36-43, <https://doi.org/10.1016/j.agwat.2013.08.003>, 2013N., Gitau, M. W., Pai,~~~~

1122 [N., and Daggupati, P.: Hydrologic and water quality models: Performance measures and evaluation](#)  
1123 [criteria, T Asabe, 58, 1763-1785, 2015.](#)

1124 Musolff, A., Schmidt, C., Selle, B., and Fleckenstein, J. H.: Catchment controls on solute export, *Adv. Water*  
1125 *Resour.*, 86, 133-146, 10.1016/j.advwatres.2015.09.026, 2015.

1126 Neitsch, S. L., Arnold, J. G., Kiniry, J. R., and Williams, J. R.: Soil and water assessment tool theoretical  
1127 documentation version 2009, Texas Water Resources Institute, 2011.

1128 ~~Ottoy, S., Elsen, A., Van De Vreken, P., Gobin, A., Merckx, R., Hermy, M., and Van Orshoven, J.: An~~  
1129 ~~exponential change decline function to estimate soil organic carbon stocks and their changes from topsoil~~  
1130 ~~measurements, European Journal of Soil Science, 67, 816-826, 2016.~~

1131 Porporato, A., D'odorico, P., Laio, F., and Rodriguez-Iturbe, I.: Hydrologic controls on soil carbon and  
1132 nitrogen cycles. I. Modeling scheme, *Advances in water resources*, 26, 45-58, 2003.

1133 Qu, Y., and Duffy, C. J.: A semidiscrete finite volume formulation for multiprocess watershed simulation,  
1134 *Water Resources Research*, 43, W08419, 2007.

1135 ~~Ranalli, A. J., and Macalady, D. L.: The importance of the riparian zone and in-stream processes in nitrate~~  
1136 ~~attenuation in undisturbed and agricultural watersheds — A review of the scientific literature, Journal of~~  
1137 ~~Hydrology, 389, 406-415, <https://doi.org/10.1016/j.jhydrol.2010.05.045>, 2010.~~

1138 Regnier, P., and Steefel, C. I.: A high resolution estimate of the inorganic nitrogen flux from the Scheldt  
1139 estuary to the coastal North Sea during a nitrogen-limited algal bloom, spring 1995, *Geochimica et*  
1140 *Cosmochimica Acta*, 63, 1359-1374, 10.1016/s0016-7037(99)00034-4, 1999.

1141 Rutherford, D. W., Chiou, C. T., and Kile, D. E.: Influence of soil organic matter composition on the partition  
1142 of organic compounds, *Environmental science & technology*, 26, 336-340, 1992.

1143 Saad, Y., and Schultz, M. H.: GMRES: A generalized minimal residual algorithm for solving nonsymmetric  
1144 linear systems, *SIAM Journal on scientific and statistical computing*, 7, 856-869, 1986.

1145 Saberi, L., ~~Crystal~~ Ng, G., ~~H-C.~~, Nelson, L., Zhi, W., ~~Li~~ L., La Frenierre, J., and Johnstone, M.:  
1146 Spatiotemporal Drivers of Hydrochemical Variability in a Tropical Glacierized Watershed in the Andes,  
1147 ~~under review~~ *Water Resources Research*, 57, e2020WR028722, 2021.

1148 ~~Saha, D., Rau, B. M., Kaye, J. P., Montes, F., Adler, P. R., and Kemanian, A. R.: Landscape control of nitrous~~  
1149 ~~oxide emissions during the transition from conservation reserve program to perennial grasses for~~  
1150 ~~bioenergy, GCB Bioenergy, 9, 783-795, doi:10.1111/gcbb.12395, 2017.~~

1151 Scudeler, C., Pangle, L., Pasetto, D., Niu, G.-Y., Volkmann, T., Paniconi, C., Putti, M., and Troch, P.:  
1152 Multiresponse modeling of variably saturated flow and isotope tracer transport for a hillslope experiment  
1153 at the Landscape Evolution Observatory, *Hydrology and Earth System Sciences*, 20, 4061-4078, 2016.

1154 Sebestyen, S. D., Ross, D. S., Shanley, J. B., Elliott, E. M., Kendall, C., Campbell, J. L., Dail, D. B., Fernandez,  
1155 I. J., Goodale, C. L., and Lawrence, G. B.: Unprocessed Atmospheric Nitrate in Waters of the Northern  
1156 Forest Region in the US and Canada, *Environmental science & technology*, 53, 3620-3633, 2019.

1157 Seibert, J., Grabs, T., Köhler, S., Laudon, H., Winterdahl, M., and Bishop, K.: Linking soil- and stream-water  
1158 chemistry based on a Riparian Flow-Concentration Integration Model, *Hydrol. Earth Syst. Sci.*, 13, 2287-  
1159 2297, 10.5194/hess-13-2287-2009, 2009.

1160 ~~Seyfried, M., Lohse, K., Marks, D., Flerchinger, G., Pierson, F., and Holbrook, W. S.: Reynolds Creek~~  
1161 ~~Experimental Watershed and Critical Zone Observatory, Vadose Zone Journal, 17, 180129,~~  
1162 ~~10.2136/vzj2018.07.0129, 2018.~~

1163 Shi, Y.: Development of a land surface hydrologic modeling and data assimilation system for the study of  
1164 subsurface-land surface interaction, 2012.

1165 Shi, Y., Davis, K. J., Duffy, C. J., and Yu, X.: Development of a coupled land surface hydrologic model and  
1166 evaluation at a critical zone observatory, *Journal of Hydrometeorology*, 14, 1401-1420, 2013.

1167 ~~Shi, Y., Eissenstat, D. M., He, Y., and Davis, K. J.: Using a spatially-distributed hydrologic biogeochemistry~~  
1168 ~~model with a nitrogen transport module to study the spatial variation of carbon processes in a Critical~~  
1169 ~~Zone Observatory, Ecological Modelling, 380, 8-21, 2018.~~

1170 Skamarock, W., and Klemp, J.: A Description of the Advanced Research WRF Model Version 4. Ncar  
1171 Technical Notes, No, NCAR/TN-556+ STR, 2019.

~~1172 Song, X., Zhang, J., Zhan, C., Xuan, Y., Ye, M., and Xu, C.: Global sensitivity analysis in hydrological modeling:  
1173 Review of concepts, methods, theoretical framework, and applications, Journal of hydrology, 523, 739-  
1174 757, 2015.~~

1175 Steefel, C., Appelo, C., Arora, B., Jacques, D., Kalbacher, T., Kolditz, O., Lagneau, V., Lichtner, P., Mayer, K.  
1176 U., and Meeussen, J.: Reactive transport codes for subsurface environmental simulation, Computational  
1177 Geosciences, 19, 445-478, 2015.

1178 Steefel, C. I., and Lasaga, A. C.: A coupled model for transport of multiple chemical species and kinetic  
1179 precipitation/dissolution reactions with application to reactive flow in single phase hydrothermal systems,  
1180 American Journal of science, 294, 529-592, 1994.

~~1181 Steimke, A. L., Han, B., Brandt, J. S., and Flores, A. N.: Climate change and curtailment: Evaluating water  
1182 management practices in the context of changing runoff regimes in a snowmelt-dominated basin, Water,  
1183 10, 1490, 2018.~~

1184 Sullivan, P. L., Hynek, S. A., Gu, X., Singha, K., White, T., West, N., Kim, H., Clarke, B., Kirby, E., Duffy, C.,  
1185 and Brantley, S. L.: Oxidative dissolution under the channel leads geomorphological evolution at the Shale  
1186 Hills catchment, American Journal of Science, 316, 981-1026, 10.2475/10.2016.02, 2016.

~~1187 Suseela, V., Conant, R. T., Wallenstein, M. D., and Dukes, J. S.: Effects of soil moisture on the temperature  
1188 sensitivity of heterotrophic respiration vary seasonally in an old-field climate change experiment, Global  
1189 Change Biology, 18, 336-348, 2012.~~

1190 Taylor, R. G., Scanlon, B., Döll, P., Rodell, M., Van Beek, R., Wada, Y., Longuevergne, L., Leblanc, M.,  
1191 Famiglietti, J. S., and Edmunds, M.: Ground water and climate change, Nature climate change, 3, 322,  
1192 2013.

~~1193 Todd, D. K., and Mays, L. W.: Groundwater Hydrology, Welly Inte, 2005.~~

1194 van der Velde, Y., de Rooij, G. H., Rozemeijer, J. C., van Geer, F. C., and Broers, H. P.: Nitrate response of  
1195 a lowland catchment: On the relation between stream concentration and travel time distribution  
1196 dynamics, Water Resources Research, 46, 10.1029/2010wr009105, 2010.

1197 van der Velde, Y., Vercauteren, N., Jaramillo, F., Dekker, S. C., Destouni, G., and Lyon, S. W.: Exploring  
1198 hydroclimatic change disparity via the Budyko framework, Hydrological Processes, 28, 4110-4118,  
1199 10.1002/hyp.9949, 2014.

1200 Weiler, M., and McDonnell, J. R. J.: Testing nutrient flushing hypotheses at the hillslope scale: A virtual  
1201 experiment approach, J. Hydrol., 319, 339-356, 10.1016/j.jhydrol.2005.06.040, 2006.

1202 Weitzman, J. N., and Kaye, J. P.: Nitrogen Budget and Topographic Controls on Nitrous Oxide in a Shale -  
1203 Based Watershed, Journal of Geophysical Research: Biogeosciences, 123, 1888-1908, 2018.

~~1204 Wen, H., and Li, L.: An upscaled rate law for magnesite dissolution in heterogeneous porous media,  
1205 Geochimica et Cosmochimica Acta, 210, 289-305, 2017.~~

~~1206 Wen, H., and Li, L.: An upscaled rate law for mineral dissolution in heterogeneous media: The role of time  
1207 and length scales, Geochimica et Cosmochimica Acta, 235, 1-20, 2018.~~

~~1208 Wen, H., Perdril, J., Bernal, S., Abbott, B. W., Dupas, R., Godsey, S. E., Harpold, A., Rizzo, D., Underwood,  
1209 K., and Adler, T.: Temperature controls production but hydrology controls export of dissolved organic  
1210 carbon at the catchment scale, 24, 945-966, 2020.~~

~~1211 Wieder, W. R., Allison, S. D., Davidson, E. A., Georgiou, K., Hararuk, O., He, Y., Hopkins, F., Luo, Y., Smith,  
1212 M. J., and Sulman, B.: Explicitly representing soil microbial processes in Earth system models, Global  
1213 Biogeochemical Cycles, 29, 1782-1800, 2015.~~

~~1214 Winter, T., Harvey, J., Franke, O., and Alley, W.: Natural processes of ground-water and surface-water  
1215 interaction, Ground Water and Surface Water: A Single Resource, US Geological Survey Circular, 1139, 2-  
1216 50, 1998.~~

1217 [Wen, H., Brantley, S. L., Davis, K. J., Duncan, J. M., and Li, L.: The Limits of Homogenization: What](#)  
1218 [Hydrological Dynamics can a Simple Model Represent at the Catchment Scale?, \*Water Resources\*](#)  
1219 [Research, 57, e2020WR029528, <https://doi.org/10.1029/2020WR029528>, 2021.](#)  
1220 Wolery, T. J.: EQ3/6, a software package for geochemical modeling of aqueous systems: package overview  
1221 and installation guide (version 7.0), 1992.  
1222 Xiao, D., Shi, Y., Brantley, S. L., Forsythe, B., DiBiase, R., Davis, K., and Li, L.: Streamflow Generation From  
1223 Catchments of Contrasting Lithologies: The Role of Soil Properties, Topography, and Catchment Size,  
1224 *Water Resources Research*, n/a, 10.1029/2018wr023736, 2019.  
1225 [Xiao, D., Brantley, S. L., and Li, L.: Vertical Connectivity Regulates Water Transit Time and Chemical](#)  
1226 [Weathering at the Hillslope Scale, \*Water Resources Research\*, 57, e2020WR029207,](#)  
1227 <https://doi.org/10.1029/2020WR029207>, 2021.  
1228 Yan, Q., Duan, Z., Mao, J., Li, X., and Dong, F.: Effects of root-zone temperature and N, P, and K supplies  
1229 on nutrient uptake of cucumber (*Cucumis sativus* L.) seedlings in hydroponics, *Soil Science and Plant*  
1230 *Nutrition*, 58, 707-717, 2012.  
1231 Yan, Z., Bond-Lamberty, B., Todd-Brown, K. E., Bailey, V. L., Li, S., Liu, C., and Liu, C.: A moisture function  
1232 of soil heterotrophic respiration that incorporates microscale processes, *Nat Commun*, 9, 2562,  
1233 10.1038/s41467-018-04971-6, 2018.  
1234 Zarnetske, J. P., Bouda, M., Abbott, B. W., Saiers, J., and Raymond, P. A.: Generality of hydrologic transport  
1235 limitation of watershed organic carbon flux across ecoregions of the United States, *Geophysical Research*  
1236 *Letters*, 45, 11,702-711,711, 2018.  
1237 Zhi, W., Li, L., Dong, W., Brown, W., Kaye, J., Steefel, C., and Williams, K. H.: Distinct Source Water  
1238 Chemistry Shapes Contrasting Concentration-Discharge Patterns, *Water Resources Research, Resour. Res.*,  
1239 55, 4233-4251, 10.1029/2018wr024257, 2019.  
1240 Zhi, W., and Li, L.: The Shallow and Deep Hypothesis: Subsurface Vertical Chemical Contrasts Shape Nitrate  
1241 Export Patterns from Different Land Uses, *Environmental Science & Technology*, 54, 11915-11928,  
1242 10.1021/acs.est.0c01340, 2020.  
1243 ~~Zhi, W., Williams, K. H., Carroll, R. W. H., Brown, W., Dong, W., Kerins, D., and Li, L.: Significant stream~~  
1244 ~~chemistry response to temperature variations in a high-elevation mountain watershed, *Communications*~~  
1245 ~~*Earth & Environment*, 1, 10.1038/s43247-020-00039-w, 2020.~~  
1246 Zhou, T., Shi, P., Hui, D., and Luo, Y.: Global pattern of temperature sensitivity of soil heterotrophic  
1247 respiration (Q10) and its implications for carbon - climate feedback, *Journal of Geophysical Research:*  
1248 *Biogeosciences*, 114, 2009.

1249

1250

1251